

Supporting Information

Rational Design of Microporous Polybenzimidazole Framework for Efficient Proton Exchange Membrane Fuel Cell

*Harilal,¹ Rama Bhattacharyya,² Avanish Shukla,³ Prakash Chandra Ghosh³ and
Tushar Jana*¹*

¹ School of Chemistry, University of Hyderabad, Hyderabad-500046, India

² Centre for Research in Nanotechnology and Science, Indian Institute of
Technology Bombay, Powai, Mumbai 400076, India

³ Department of Energy Science & Engineering, Indian Institute of
Technology Bombay, Mumbai, 400076, India

(* To whom correspondence should be addressed)

Tel: (91) 4023134808 Fax: (91) 4023012460

Email: tusharjana@uohyd.ac.in

tjscuoh@gmail.com

Section S1. Materials

Phosphorus pentoxide (P₂O₅), hydroquinone, 2-phenylhydroquinone, anthracene, sodium bicarbonate, sodium dithionite, palladium on carbon (Pd/C, 10 wt %), hydrazine monohydrate and 2-methylhydroquinone were obtained from Sigma-Aldrich and used as received. Acetic acid (99.5%), dimethyl acetamide (DMAc), dimethyl sulphoxide (DMSO), *N*-methyl-2-pyrrolidone (NMP), methane sulfonic acid (CH₃SO₃H), sulphuric acid (99.8%), Trifluoromethanesulfonic acid (TFSA), and orthophosphoric acid (85%) were purchased from Finar, India and used as received. Ammonium acetate (96%), acetic anhydride (97%), hydrogen peroxide (H₂O₂) and 4-fluorobenzonitrile, hydrazine monohydrate was obtained from Fisher Scientific. The NMR solvent dimethyl sulfoxide (DMSO-*d*₆) was obtained from Sigma-Aldrich used without additional purification. 2,6-bis(3',4'-diaminophenyl)-4-phenylpyridine (PyTAB) was synthesized by following our earlier reported procedure¹ and characterized by NMR (¹H and ¹³C) spectroscopy (**Figure S1**).

Section S2. Instrumentation and methods

Viscosity measurement

The inherent viscosity (I.V) of the polymer solutions was measured using a Cannon Ubbelohde capillary dilution viscometer (model F725) at 30 °C. All the polymers [Trip-PyPBI, Trip(CH₃)-PyPBI, PenTrip-PyPBI and PenTrip(CH₃)-PyPBI] were dissolved in 98% sulphuric acid at a concentration of 0.2 g/dL. The insoluble precipitate was passed through a 0.25 μm PTFE syringe filter before injecting into the viscometer. The I.V values were determined from the flow time data by using eq. (1)

$$IV = \frac{\ln\left(\frac{t}{t_0}\right)}{c} \quad (1)$$

Where C is the polymer solution concentration of 0.2 g/dL, and t and t₀ are the flow times of the polymer solution and sulphuric acid, respectively. The reproducibility in measuring IV was assessed and the relative error for this technique was found to be <1%.

Stability test

All the polymer membranes including Ph-PyOPBI membrane were immersed into H₃PO₄ (85%) for 72 h at 100 °C. Then the samples were taken out and washed with deionized water for several times. Finally, the membranes were dried for 24 h at 110 °C. The weight losses were obtained by weighing the membranes before and after solubility test. The remaining weight was calculated by the following eq. (2)

$$\text{Remaining weight} = \frac{W_b - W_a}{W_b} \times 100\% \quad (2)$$

Where W_b and W_a are the weight of dry membranes before and after being immersed in phosphoric acid (PA), respectively.

Powder X-ray Diffraction (PXRD)

The PXRD patterns of all polymer membrane samples were recorded using a Rigaku Philips (model PW 1830) powder diffraction instrument. The samples were placed on a glass slide, and the diffractograms were recorded with nickel-filtered Cu-K_α radiation source ($\lambda = 1.5406 \text{ \AA}$) operated at 40 kV and 50 mA current in the 2 θ range of 5-100° with a scanning rate of 0.6° 2 θ /min at room temperature.

Single Crystal X-ray Diffraction (SC-XRD)

All the newly synthesized diacids were recrystallized from 1, 4-dioxane at room temperature. Single crystal X-ray data for crystals of compounds: Trip-COOH, Trip(CH₃)-COOH, PenTrip-COOH and PenTrip(CH₃)-COOH were recorded on a Rigaku Oxford Diffraction CCD single crystal diffractometer using graphite monochromatic Mo K_α ($\lambda = 0.71073 \text{ \AA}$) radiation at 293 K whereas Trip(CH₃)-COOH was collected at 104 K. Unit cell

measurement, data collection, integration, scaling, and absorption corrections were performed using Rigaku Oxford Diffraction. Multiscan absorption corrections were applied using SADABS-2014. The structure was solved by direct methods using SHELXS-97 and refined with the full matrix least squares method using SHELXL-2021² present in the program Olex2-1.3-ac4 software. All of the non-hydrogen atoms were refined anisotropically. Hydrogen atoms on the O atoms were located by Fourier map refinement and further DFIX command was employed for some of the hydrogen atoms to fix in their calculated positions. Due to solvent disorder, B alerts are found in IUCR checkcif report for the two structures **8d** (CCDC 1951204) and **4c** (CCDC 2099945). Further, to understand the presence of disordered residual solvent (dioxane) in the void space of **4c** (CCDC 2099945) crystal structure was confirmed by the TGA analysis. Experimental weight loss of 20.31% (shown in Fig. S36) was observed for **4c** which is constituent with the calculated weight percentage (20.02%). From the derivative curve of the Fig. S36, the weight loss was observed from 55 to 150 °C, which can be attributed to the loss of residual solvent (1,4-Dioxane). The packing diagram of the crystal was generated using *Mercury* software. All the crystal structures, the fully refined final structures, were deposited to CCDC and the crystallographic parameters are summarized in **Table S1(a)** and **S1(b)**. In addition, full crystallographic details can be obtained free of charge from the Cambridge Crystallographic Data Center (CCDC) via www.ccdc.cam.ac.uk/data_request/cif (CCDC 2099945, 2070350, 2070384 and 1951204 for **4c**, **4d**, **8c** and **8d**, respectively).

BET adsorption

N₂ gas adsorption experiment (up to 1 bar) of polymers were performed on a Quantachrome Quadrasorb automatic gas adsorption analyzer. Prior to surface area analysis, the samples were activated at 120 °C for 20 hours. The porosity of polymer networks were measured by N₂ adsorption-desorption of an activated sample at 77 K. The Brunauer-Emmett-Teller (BET) surface area of the polymers were determined by multipoint BET analysis.

Thermogravimetric analysis (TGA)

The thermal performance was measured by thermogravimetric analysis (TGA) curves with a TGA (TGA Q-500, TA instruments) instrument in the presence of N₂ atmosphere at a flow rate of 50 mL min⁻¹. TGA profiles of membranes were collected over a temperature range between 30 °C to 700 °C with a scanning rate of 10 °C /min⁻¹. Each polymer sample was taken approximately 5-10 mg in these experiments and tested for at least 3 times.

Dynamic mechanical analysis (DMA)

The thermo-mechanical properties of prepared membranes were performed using a dynamic mechanical analyser (DMA, Q-800, TA Instruments) under a tensile mode from 100 to 450 °C at a heating rate of 3 °C min⁻¹. Prior to the test, the membrane samples were equilibrated at 100 °C overnight to remove the water from the membrane. The oscillation frequency was set 1Hz. The membrane samples were cut into a rectangular form having dimension of (35 × 10 × 2 mm) using a knife and data was collected for at least 3 times.

Absorption spectroscopy

Absorption spectra were recorded on a JASCO (V-750) UV-visible spectrometer. All the polymers were dissolved in DMSO and the spectra were recorded. The concentration of the sample solutions was taken 1mg/mL.

Oxidative stability

The oxidative stability of the polymer membranes was performed via Fenton test (3% H₂O₂ solution with 4 ppm Fe²⁺ ions) at 70 °C for every 24 h. The sample strips were put into Fenton's reagent and taken out every 24 h. After drying for 24 h, the weight of each piece of membranes were taken to detect the weight change.

Field emission scanning electron microscopy (FE-SEM)

The cross-sectional morphology images of the fracture prepared membranes were observed through FE-SEM (Carl Zeiss Ultra-55 using EHT detector at accelerating voltage of 5 kV) analysis. Before cross-sectional analysis, all membrane samples were cryogenically fractured in liquid nitrogen. Prior to the measurements, all samples sputtered with a thin film of gold to avoid charging effects during SEM analysis.

Transmission electron microscopy (TEM)

Transmission electron microscopy images were collected using a JEOL JEM-2100 TEM equipped with a thermal LaB₆ gun, operated at an acceleration voltage of 200 kV. The images were recorded using a Gatan Orius SC200D CCD camera. The samples were prepared by placing a drop of DMSO polymer solution on carbon coated copper (200 mesh) grids and dried overnight at 120 °C for 48 h.

Atomic force microscope (AFM)

AFM studies were carried out on NT-MDT Model Solver Pro M microscope using a class 2R laser of 650 nm wavelength having a maximum output of 1 mW. All calculations and image processing were carried out by using NOVA 1.0.26.1443 software provided by the manufacturer. The images were recorded in tapping mode using a super sharp silicon cantilever (NSG 10-DLC) with a diamond-like carbon tip (NT-MDT, Moscow).

ATR-FTIR and NMR analysis

The attenuated total reflection-Fourier transform infrared (ATR-FTIR) spectra were collected in a transmission configuration on a Nicolet iS50 FTIR instrument (Thermo Fisher) with a wavenumber ranging from 400 to 4000 cm⁻¹ at 25 °C to confirm the structure of the synthesized membranes. Nuclear magnetic resonance (¹H NMR) analyses were carried out

using a Bruker-500 NMR 500 MHz spectrophotometer (Advance III, Bruker, Switzerland), and DMSO- d_6 and tetramethyl silane (TMS) were used as a solvent and as an internal chemical shift reference, respectively. Solid-state ^{13}C CPMAS NMR spectra were obtained at ambient temperature with Bruker AV 400 MHz NMR spectrometer operating at 500 MHz at a spinning rate of 5 kHz and a contact time of 2 ms.

Phosphoric acid (PA) doping (loading)

The PA doping process of the membranes were performed in 85 wt% phosphoric acid (PA) reservoir until equilibrium sorption occurred. Specifically, five dried membranes of each type of PyPBI membranes were cut in $4 \times 4 \text{ cm}^2$ size specimens and the weights of individual specimens were separately noted. The specimens were immersed in a phosphoric acid aqueous solution at $30 \text{ }^\circ\text{C}$ for 3 days. The acid doped membranes were removed from the PA, wiped the specimens many times using tissue paper, and then titrated against NaOH using an Automated Metrohm 702 titrator. The PA doping level was calculated as the number of moles of PA per repeating unit of polymer using the equation (3) where M_{PA} , $M_{polymer}$ refer the molecular weight of phosphoric acid and repeat unit of the polymer component, respectively. W_{doped} and $W_{undoped}$ are the weights of polymer membrane after and before doping with PA, respectively.

$$\text{PA doping level (mole/repeat unit of polymer)} = \frac{(W_{doped} - W_{undoped}) / M_{PA}}{(W_{undoped}) / M_{polymer}} \quad (3)$$

Swelling ratio in PA and water were also measured and calculated using the equation (4)

$$\text{Swelling ratio in PA and water (\%)} = \frac{L_d - L_u}{L_u} \times 100\% \quad (4)$$

Where L_d and L_u represent the lengths of doped and undoped samples, respectively

Proton conductivity

Proton conductivities of the membranes were measured by a four-probe electrochemical alternating current impedance spectroscopy method using a Metrohm model

PGSTAT302N Autolab analyser over a frequency range of 100 m Hz to 1 MHz. A rectangular size (1.5 cm × 4.0 cm) membranes were sandwiched between two platinum electrodes. The conductivity was measured from 30 °C to 180 °C at every 20°C interval under anhydrous conditions. Before the measurement, the membranes were dried in a vacuum oven at 100 °C for 2 hours so as to ensure the complete removal of water molecules from the membrane. Samples were kept at each measurement temperature for 30 minutes so that temperature equilibrium is reached. The reproducibility of the impedance measurement was checked by repeating the experiment at least three times for all the samples studied here. Finally, proton conductivity of the membranes (σ) was calculated using the following equation

$$\sigma = D/RTW \quad (5)$$

Where, D is the space (cm) between counter and working electrodes, T is the thickness of the membrane, W is the width of the membrane, R is the Ohmic resistance obtained from the Nyquist plots (**Figure S37**) of the impedance measurements.

Acid retention test

The acid leaching test was performed for the membrane of iptycene-based PyPBI membranes according to the previous reports.¹⁰ The phosphoric acid (PA) loaded membranes were taken out from the acid bath medium and excess PA was removed by wiping with a tissue paper. The membranes were then placed under the vapour condition at 100 °C for a period of three hours and the weight of the membrane (W_t) after every 30 minutes was recorded after removing the leached acid from the membrane. The weight loss percentage ratio of acid in the membranes was calculated by using the following formula:

$$\text{Remaining weight} = \frac{W_o - W_t}{W_a} \times 100\% \quad (6)$$

Where, W_o is weight of the PA doped membranes at the initial time of zero hour, W_t is the weight of the PA membrane after leaching at different times (t) and W_a is the original weight of PA present in the membranes calculated from the PA doping level of the membranes.

Fabrication of membrane electrode assembly (MEA)

The MEA were fabricated comparable to the method reported elsewhere³⁵. In brief, the catalyst slurry was prepared by 40 wt% platinum supported on carbon using solvent as iso-propyl alcohol and 10 wt% poly-tetrafluoroethylene (PTFE) solution as binder. The electrodes were fabricated by brush coating of the above prepared slurry on the commercial gas diffusion layer with loading of 0.6 mg cm⁻². Further the synthesized membrane was uni-axially sandwiched between the electrodes to form MEA.

Fuel cell performance evaluation

MEA was assembled in a single cell (indigenously engineered) with 2 cm² serpentine flow field area made up of graphite plates along with current collector and end plates. The cell was further stabilized/activated for 1 h and then tested for polarization (I-V characteristics). High pure H₂ and O₂ with the stoichiometry of 1.2 and 3 at ambient pressure were supplied as a fuel and oxidant on anode and cathode side respectively for HT-PEM-FC test. Polarization experiments were carried out at 160 °C after stabilizing the fuel cell in an DC electronic load PRODIGIT Instrument Professional, Taiwan (Model: 3354F).

Section S3. Synthetic procedural information and characterization data for monomers

Synthesis of pentiptycene quinone (1)

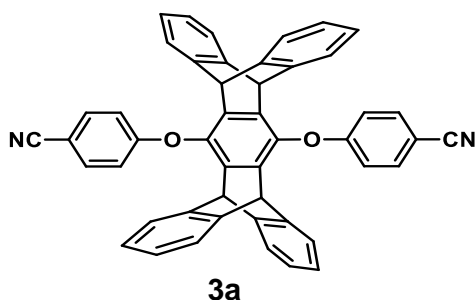
Compound (1) was synthesized using modified literature procedure.^{3, 4} A mixture of anthracene (0.04 mol, 7.1 g), p-benzoquinone (0.024 mol, 2.6g) and tetra-chloro-1,4-benzoquinone (0.04 mol, 9.8 g) in 250 mL of glacial acetic acid (AcOH) was refluxed for 16 h. After cooling to room temperature, the solid was filtered, washed several times with diethyl ether and AcOH and then dried under reduced pressure at room temperature to get 8.4 g (yield

= 91%) of pentiptycene quinone as a yellow solid. The structure was confirmed by ^1H and ^{13}C NMR (CDCl_3) as shown in **Figure S2**.

Synthesis of pentiptycene hydroquinone (2)

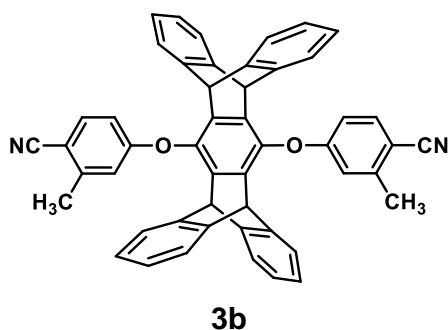
Compound (2) was synthesized using modified literature procedure.^{3, 4} 8.1 g (0.018 mol) of the synthesized pentiptycene quinone (1) was dissolved in 170 mL of DMF followed by the addition of 0.125 mol (10.5 g) of sodium bicarbonate and 0.061 mol (10.5 g) of sodium dithionite. The mixture was stirred at 100°C for 18 h during which time three additional portions of 10.5 g of sodium bicarbonate were added for further reduction. The solution was cooled to room temperature and poured into 500 mL of water. The white precipitated pentiptycene diol was collected, washed several times with water and dried under reduced pressure (yield = 98%). ^1H and ^{13}C NMR (CDCl_3) of the synthesized compound are shown in **Figure S3**.

Synthesis of pentiptycene containing dicyano compounds (3a and b)



Compound 3a: The detailed synthetic route for the synthesis of 1,4-bis(cyanophenoxy) pentiptycene (PenTrip-CN) **3a** is elaborated here as a representative one. Similar procedure was followed for **3b** with appropriate reactant as shown in **Scheme 1** in the main article. Pentiptycene hydroquinone **2** (7.1 g, 15.1 mmol) and 4-fluoro benzonitrile (4.33 g, 35.7 mmol) were dissolved in dry DMF (40 mL) in a 100 mL two-necked round-bottom flask followed by the addition of K_2CO_3 (4.03 g, 29.1 mmol) under N_2 atmosphere. After refluxing at 150°C under N_2 atmosphere for 6 h, the solvent (DMF) was removed under vacuum and the resultant solid dicyano compound was obtained and washed with acetone and deionized (DI) water extensively and dried at 100°C in

a vacuum oven overnight to obtain a white powder as the dicyano compound **3a** (PenTrip-CN) (9.1 g, yield 90%) m.p [melting point obtained from differential scanning calorimetry at a heating rate of 2 °C min⁻¹]: 491 °C. ¹H NMR (400 MHz, CDCl₃) δ [ppm]: 7.66 (d, *J* = 8.8 Hz, 4H), 7.29 (s, 1H), 7.09 (dd, *J* = 5.2, 3.3 Hz, 8H), 6.94 (dd, *J* = 5.3, 3.1 Hz, 8H), 6.88 (d, *J* = 8.8 Hz, 4H), 5.39 (s, 4H) (**Figure S4**). ¹³C NMR (101 MHz, CDCl₃) δ [ppm]: 162.02, 144.08, 141.06, 137.86, 134.55, 125.54, 123.83, 118.90, 116.51, 105.88, 77.36, 77.04, 76.72, 48.18 (**Figure S4**). HRMS (m/z) for C₄₈H₂₈N₂O₂ [M+Na⁺]: Calcd 687.1901; Found 687.1903. IR (ATR) [wavenumber (ν), cm⁻¹] = 3018, 2224, 1600, 1500, 1457, 1297, 1228, 1164, 987, 826, 739, 595 (**Figure S5**).

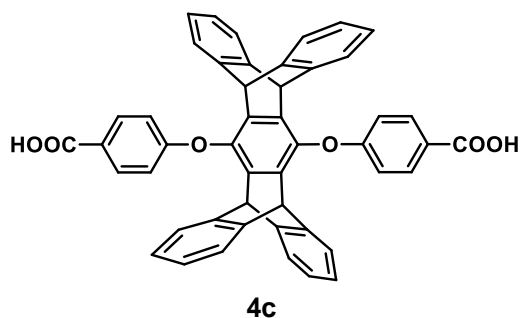


Compound 3b: It should be noted that a similar procedure was followed for the synthesis of the 1,4-bis(cyanophenoxy) 2-methyl pentiptycene product [PenTrip(CH₃)-CN] **3b** (yield 87%), mp: 444 °C by DSC at 2 °C/min. ¹H NMR (400 MHz, CDCl₃) δ [ppm]: 7.57

(d, *J* = 8.6 Hz, 2H), 7.29 (s, 1H), 7.10 (dd, *J* = 5.2, 3.2 Hz, 8H), 6.94 (dd, *J* = 5.3, 3.1 Hz, 8H), 6.75 (d, *J* = 1.9 Hz, 2H), 6.64 (dd, *J* = 8.5, 2.3 Hz, 2H), 5.39 (s, 4H), 2.49 (s, 6H) (**Figure S6**). ¹³C NMR (101 MHz, CDCl₃) δ [ppm]: 161.79, 144.87, 144.15, 141.05, 137.72, 134.76, 125.46, 123.86, 118.27, 117.31, 113.74, 106.39, 77.35, 77.04, 76.72, 48.19, 20.66 (**Figure S6**). HRMS (m/z) for C₅₀H₃₂N₂O₂ [M+1]: Calcd 693.25; Found 693.2544. IR (ATR): ν [cm⁻¹] = 3084, 2225, 1611, 1576, 1498, 1437, 1322, 1302, 1227, 1170, 1117, 1044, 994, 961, 918, 890, 837, 790, 740, 707, 636, 594 (**Figure S7**).

Synthesis of pentiptycene containing diacid monomers (**4c** and **d**)

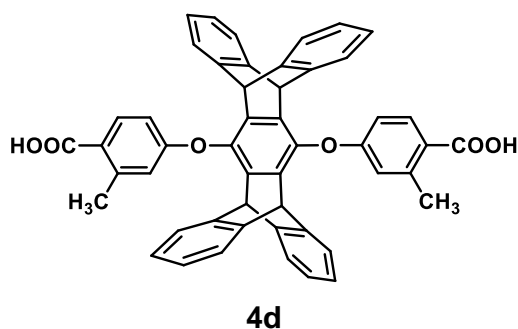
Monomer 4c: We screened various synthetic conditions which include solvents, temperature



and reaction time (**Table S2**) to make the diacid monomers in good yield. 4,4'-((5,7,12,14-tetrahydro-5,14:7,12-bis([1,2]benzeno)pentacene-6,13-diyl)bis(oxy))dibenzoic acid (PenTrip-COOH) **4c** was finally obtained under optimal

synthetic condition as discussed below. The dicyano-para product **3a** (20 g, 0.1 mmol) and triethylene glycol (250 mL) were placed in a 500 mL one-neck round-bottomed flask equipped with a magnetic stirrer and the mixture was refluxed at 200 °C for approximately 10 h to form a homogeneous solution. The resulting clear solution was cooled down to room temperature and aqueous KOH solution (44 g KOH in 200 mL H₂O) was added. Furthermore, the reaction mixture was refluxed under stirring for approximately 24 h at 100 °C. The mixture was allowed to cool to room temperature and the solution was slowly acidified with concentrated hydrochloric acid (HCl) through an addition funnel with ice bath until the solution reached a pH=1. Then, the mixture was stirred for another 1 hour. Thereafter, the white precipitate was filtered and washed repeatedly with deionized (DI) water, and then dried for 24 h at 140 °C until constant weight. The obtained white powder was recrystallized twice with dioxane to afford PenTrip-COOH (**4c**) as colorless crystals (12.6 g, 80% yield; m.p 373 °C by DSC at 2 °C/min). **¹H NMR** (500 MHz, DMSO-*d*₆) δ [ppm]: 12.85 (s, 2H), 7.97 – 7.92 (m, 6H), 7.27 (dd, *J* = 5.3, 3.2 Hz, 6H), 7.00 (dd, *J* = 5.4, 3.1 Hz, 6H), 6.96 – 6.94 (m, 5H), 6.88 (s, 2H), 5.69 (s, 4H) (**Figure S8**). **¹³C NMR** (101 MHz, DMSO-*d*₆) δ [ppm]: 167.27, 162.26, 144.59, 141.57, 138.08, 132.26, 125.75, 125.60, 124.21, 115.99, 47.80 (**Figure S8**). **HRMS** (*m/z*) for C₄₈H₃₀O₆ [*M*+1]: calcd 703.20; found, 703.2122. **IR (ATR):** ν [cm⁻¹] = 2978, 1689, 1603, 1459, 1422, 1219, 1161, 989, 798, 747, 580, 550. The structure of PenTrip-COOH (**4c**) was also determined

and confirmed by single crystal x-ray diffraction (SCXRD) analysis and the obtained structure is shown in **Scheme 1** in the main article. The crystallographic data are shown in **Table S1(a)**.



Monomer 4d: The synthetic procedure 4,4'-

((5,7,12,14-tetrahydro-5,14:7,12-

bis([1,2]benzeno)pentacene-6,13-

diyl)bis(oxy))bis(2-methylbenzoic acid)

(PenTrip(CH₃)-COOH) **4d** was the same as that of

PenTrip-COOH (**4c**) except that in this case PenTrip(CH₃)-CN (**3b**) intermediate was used for the acid hydrolysis. The resulting monomer was obtained as white solid and then crystallized from dioxane to afford PenTrip(CH₃)-COOH (**4d**) as colorless crystals (12.6 g, 80% yield, m.p: 377 °C by DSC at 2 °C/min). ¹H NMR (400 MHz, DMSO-*d*₆) δ [ppm]: ¹H NMR (400 MHz, DMSO-*d*₆) δ 12.78 (s, 2H), 7.91 (d, *J* = 8.7 Hz, 2H), 7.17 – 7.11 (m, 8H), 6.93 (dd, *J* = 5.3, 3.1 Hz, 8H), 6.65 (dd, *J* = 8.6, 2.3 Hz, 2H), 6.55 (d, *J* = 2.1 Hz, 2H), 5.54 (s, 4H), 2.40 (s, 6H) (**Figure S9**). ¹³C NMR (101 MHz, DMSO-*d*₆) δ [ppm]: 168.38, 160.98, 144.58, 142.96, 141.44, 138.04, 125.71, 124.77, 124.29, 118.60, 113.30, 47.80, 22.21 (**Figure S9**). IR (ATR): ν [cm⁻¹] = 2980, 1681, 1600, 1459, 1227, 1142, 990, 860, 752, 691, 580, 447. The structure of PenTrip(CH₃)-COOH (**4d**) was also determined and confirmed by single crystal x-ray diffraction (SCXRD) data [**Scheme 1** and **Table S1(a)**].

Synthesis of triptycene quinone (**5**)

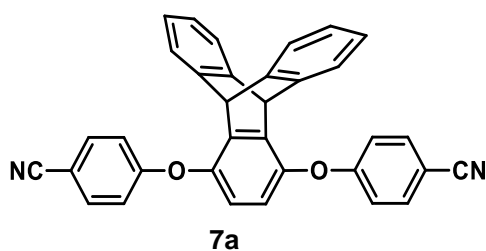
Triptycene quinone (**5**) was prepared according to the published literature.³ A typical reaction is as follows: anthracene (10.12 g, 56.67 mmol), *p*-benzoquinone (7.37 g, 68.14 mmol) and xylenes (70.8 mL) were added into a round-bottom flask with a stir bar. The mixture was refluxed at 140 °C under stirring in a nitrogen atmosphere for six hours. The mixture was

allowed to cool to room temperature and then filtered. The obtained solid was then washed three times with hot water (500 mL). The quinone product (**5**) (13.02 g, 80% yield) was collected and dried at 60 °C under vacuum overnight. The structure was confirmed by ¹H and ¹³C NMR (CDCl₃) spectra (**Figure S10**).

Synthesis of triptycene hydroquinone (**6**)

To synthesize triptycene hydroquinone (**6**), the quinone product (**5**) (13.02 g, 45.4 mmol) and glacial acetic acid (165 mL) were added into a round-bottom flask with a stir bar. The mixture was brought to reflux at 118 °C under a nitrogen atmosphere. Hydrobromic acid (HBr, 48%) (0.7 mL) was added to the flask and the mixture was allowed to reflux for an additional 30 minutes. A light tan precipitate was formed. The mixture was allowed to cool to room temperature and then filtered. The resulting hydroquinone product (**6**) (11.71 g, 90% yield) was dried under vacuum at 60 °C for 9 hours. The structure was confirmed by ¹H and ¹³C NMR spectra as shown in **Figure S11**.

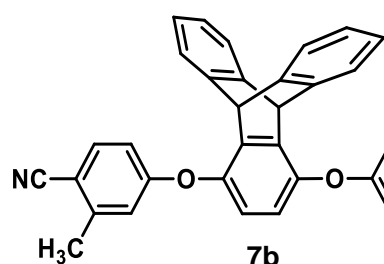
Synthesis of triptycene containing dicyano compounds (**7a** and **7b**)



Compound 7a and **7b**: The dicyano compounds 1,4-bis(cyanophenoxy) triptycene (Trip-CN) **7a** and 1,4-bis(cyanophenoxy) 2-methyl triptycene (Trip(CH₃)-CN) **7b** were synthesized

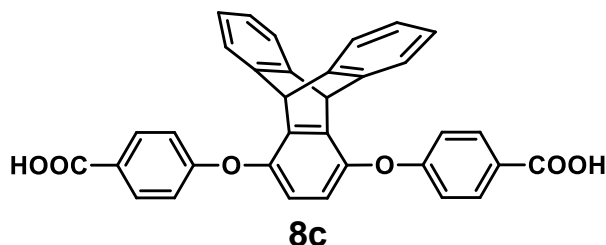
following the similar procedure used for **3a** and **3b**. The resulting mixtures were poured into the acetone and water (v/v = 1:1), filtered, washed and dried under vacuum at 100 °C overnight giving a white powder as dicyano compounds **7a** and **7b**, respectively. **7a** (Trip-CN): (Yield: 90%), mp. 330 °C by DSC at 2 °C/min. ¹H NMR (400 MHz, DMSO-*d*₆) δ [ppm]: 7.80 (s, 1H), 7.78 (s, 1H), 7.25 (dd, *J* = 5.3, 3.2 Hz, 4H), 7.03 (dd, *J* = 5.4, 3.2 Hz, 4H), 6.93 (s, 2H), 6.86

(d, $J = 2.5$ Hz, 2H), 6.84 (d, $J = 2.5$ Hz, 1H), 6.81 (d, $J = 2.4$ Hz, 1H), 5.61 (s, 2H), 2.40 (s, 6H) (**Figure S12**). ^{13}C NMR (101 MHz, CDCl_3) δ [ppm]: 162.02, 144.08, 141.06, 137.86, 134.55, 125.54, 123.83, 118.90, 116.51, 105.88, 48.18 (**Figure S12**). HRMS for $\text{C}_{34}\text{H}_{20}\text{N}_2\text{O}_2$ [$\text{M}+\text{NH}_4^+$]: Calcd 506.19; Found 506.1883. IR (ATR): ν [cm^{-1}] = 3071, 2222, 1600, 1502, 1470, 1232, 1210, 1161, 991, 828, 791, 730, 635, 539 (**Figure S13**).



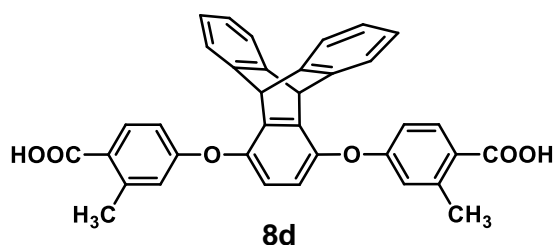
Compound 7b: Yield 90%. mp: 317 °C by DSC at 2 °C/min. ^1H NMR (400 MHz, $\text{DMSO}-d_6$) δ [ppm]: 7.80 (s, 1H), 7.78 (s, 1H), 7.25 (dd, $J = 5.3$, 3.2 Hz, 4H), 7.03 (dd, $J = 5.4$, 3.2 Hz, 4H), 6.93 (s, 2H), 6.86 (d, $J = 2.5$ Hz, 2H), 6.84 (d, $J = 2.5$ Hz, 1H), 6.81 (d, $J = 2.4$ Hz, 1H), 5.61 (s, 2H), 2.40 (s, 6H) (**Figure S14**). ^{13}C NMR (101 MHz, $\text{DMSO}-d_6$) δ 161.60, 146.11, 144.83, 144.37, 140.00, 135.32, 128.99, 125.92, 124.55, 120.32, 118.40, 115.03, 106.15, 48.00, 20.52 (**Figure S14**). HRMS (m/z) for $\text{C}_{36}\text{H}_{24}\text{N}_2\text{O}_2$: Calcd 516.16; Found 516.1689. IR (ATR): ν [cm^{-1}] = 3071, 2212, 1599, 1566, 1466, 1281, 1240, 1211, 1161, 1098, 1016, 946, 863, 814, 736, 699, 635, 585 (**Figure S15**).

Synthesis of triptycene containing diacid monomers (**8c** and **8d**)



Monomers 8c and 8d: The diacid compounds 4,4'-((9,10-dihydro-9,10-[1,2]benzenoanthracene-1,4-diyl)bis(oxy))dibenzoic acid (Trip-COOH) **8c** and 4,4'-((9,10-dihydro-9,10-[1,2]benzenoanthracene-1,4-diyl)bis(oxy))bis(2-methylbenzoic acid) (Trip(CH_3)-COOH) **8d** were synthesized following the similar procedure used for PenTrip-COOH (**4c**) and

PenTrip(CH₃)-COOH (**4d**). The resulting mixtures were acidified with HCl at pH 1 and the white precipitate was filtered, washed with water, dried at 140 °C, and then crystallized from dioxane to afford Trip-COOH (**8c**) and Trip(CH₃)-COOH (**8d**) as colorless crystals, respectively. **8c** (Trip-COOH) (6.0 g, 80% yield; mp 385-388 °C, by DSC at 2 °C/min). ¹H NMR (500 MHz, DMSO-d₆) δ [ppm]: 12.85 (s, 2H), 8.06 – 7.88 (m, 4H), 7.27 (dd, *J* = 5.3, 3.2 Hz, 4H), 7.07 – 6.98 (m, 4H), 7.00 – 6.92 (m, 4H), 6.88 (s, 2H), 5.69 (s, 2H) (**Figure S16**). ¹³C NMR (126 MHz, DMSO-d₆) δ [ppm]: 167.29, 161.95, 146.58, 144.63, 144.45, 139.82, 132.18, 125.87, 125.72, 124.47, 120.10, 117.74, 116.83, 47.63 (**Figure S16**). HRMS (*m/z*): [M]⁺ calcd. for C₃₄H₂₂O₆, 526.14; found, 526.2264. IR (ATR): ν [cm⁻¹] = 2960, 1687, 1600, 1458, 1421, 1286, 1218, 1161, 1099, 851, 798, 746, 686, 549, 500, 458, 420. The structure of Trip-COOH was also determined by single crystal x-ray diffraction (SCXRD) data [**Scheme 1**, **Table S1(b)**].



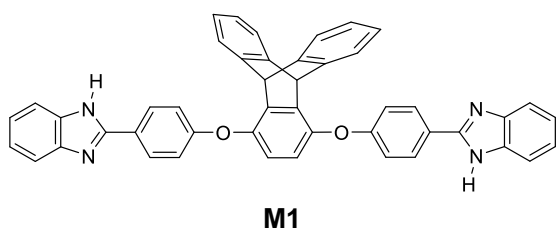
8d (Trip(CH₃)-COOH): Yield: 80%, m.p. 323 °C by DSC at 2 °C/min. ¹H NMR (500 MHz, DMSO-*d*₆) δ [ppm]: 12.68 (s, 2H), 7.88 (d, *J* = 8.6 Hz, 2H), 7.26 (dd, *J* = 5.3, 3.2 Hz, 4H), 7.10 – 6.93 (m, 6H), 6.85 (d, *J* = 4.6 Hz, 2H), 6.73 (ddd, *J* = 19.0, 10.0, 3.6 Hz, 4H), 5.65 (s, 2H), 2.45 (s, 6H) (**Figure S17**). ¹³C NMR (126 MHz, DMSO-*d*₆) δ [ppm]: 168.34, 146.50, 144.56, 133.46, 125.81, 124.51, 120.00, 119.50, 114.15, 47.74, 22.07 (**Figure S17**). HRMS (*m/z*) for C₃₆H₂₆O₆ [M+1]: calcd, 554.1815; found, 554.1815. IR (ATR): ν [cm⁻¹] = 2919, 2847, 1671, 1596, 1471, 1319, 1216, 1141, 990, 862, 777, 741, 710, 618, 509, 438. The structure of Trip(CH₃)-COOH (**8d**) was also determined and confirmed by single crystal x-ray diffraction (SCXRD) data [**Scheme 1** and **Table S1(b)**].

Section S4. Preparation of Eaton's Reagent

36 g of P₂O₅ and 360 g of MSA were placed in a 500 mL flask fitted with a mechanical stirrer. The mixture was stirred at 50 °C until the P₂O₅ was completely dissolved. The reagent was sealed and stored for later use. In short this reagent is called as PPMA (mixture of P₂O₅ and MSA).⁵

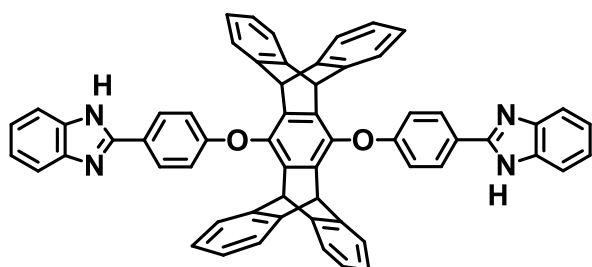
Section S5. Synthetic procedural information and characterization data for model compounds

Synthesis of model compounds



Compound M1: A 25 mL three neck round-bottom flask was charged with 2.0 g (2.8 mmol) of purified PenTrip(CH₃)-COOH and 0.6 g (5.5 mmol) of o-Phenylenediamine (OPDA) in a reaction medium consisting of a mixture of PPMA (1:1 mixture of P₂O₅ and CF₃SO₃H) and CH₃SO₃H (TFSA) under inert atmosphere. Afterward, the mixture was stirred using overhead mechanical stirrer and gradually heated up to 100 °C for 2 h and another 1 h stirring was continued at 140 °C under nitrogen atmosphere. Thereafter, a homogeneous solution was obtained immediately and a viscosity increase was observed. After the complete reaction, a dark brown colour viscous solution was slowly poured into deionized (DI) water with stirring and the collected precipitated model compounds (**M1**) was filtrated and washed with copious amount of DI water several times. The residual phosphoric acid in the product powder was neutralized with 10 wt % sodium hydrogen carbonate (NaHCO₃) solution at 40 °C overnight and the **M1** was washed thoroughly with DI water until the wash water pH reached 7.0 and then dried under reduced pressure at 100 °C for 24 h to get 2.1 g (95% yield) of a dark brown

solid (see **Figure 1a** in the main article). $^1\text{H NMR}$ (400 MHz, $\text{DMSO-}d_6$) δ [ppm]: 13.57 (s, 1H), 8.23 (s, 2H), 8.05 (s, 2H), 7.94 (d, 6H), 7.78 (s, 2H), 7.62 (t, 3H), 7.37 (s, 2H), 7.23 (d, 6H), 6.99 (s, 2H), 6.16 (s, 2H) (**Figure S18**). $^{13}\text{C CP-MAS solid-state NMR}$ (400 MHz) δ [ppm]: 151.32, 146.57, 141.48, 138.44, 136.88, 131.63, 130.04, 128.07, 127.35, 126.48, 125.48, 124.96, 124.26, 122.28, 120.94, 119.94, 49.45 (**Figure S18**). **IR (ATR):** ν [cm^{-1}] = 3065 (imidazole ring N–H vibration), 1601-1472 (C=N, C=C vibration), 1304 (in-plane benzimidazole ring vibration), 1226-1168 (asymmetric C–O vibration) (**Figure S19**).



M2

Compound M2: The procedure (see

Figure 1a in the main article) to prepare **M2**

was similar to that used for **M1**. $^1\text{H NMR}$ (500

MHz, $\text{DMSO-}d_6$) δ [ppm]: 13.48 (s, 1H), 8.28

(d, 2H), 8.08 (d, 4H), 7.96 (m, 8H), 7.80 (d,

2H), 7.54 (d, 4H), 7.48 (d, 4H), 7.29 (d, 2H), 7.03 (d 2H), 6.75 (m, 4H), 6.08 (s, 4H) (**Figure**

S20). $^{13}\text{C CP-MAS solid-state NMR}$ (400 MHz) δ [ppm]: 151.32, 146.57, 140.95, 138.44,

136.88, 131.63, 130.04, 128.07, 127.35, 126.48, 125.48, 124.96, 124.26, 122.28, 120.94,

119.94, 118.22, 116.58, 112.84, 49.45 (**Figure S20**). **IR (ATR):** ν [cm^{-1}] = 2924 (imidazole

ring N–H vibration), 1602-1456 (C=N, C=C vibration), 1410-1304 (in-plane benzimidazole

ring vibration), 1212-1133 (asymmetric C–O vibration) (**Figure S21**).

Section S6. Crystallographic data for monomers

Table S1 (a). Crystallographic data and structure refinement for PenTrip-COOH and PenTrip(CH₃)-COOH.

Sample code	PenTrip-COOH (4c)	PenTrip(CH ₃)-COOH (4d)
Crystal system	monoclinic	triclinic
Space group	P 1 21/c 1	P-1
Chemical formula	C ₅₂ H ₃₈ O ₈	C ₇₀ H ₇₄ O ₁₆
Formula weight	790.82	1171.29
Radiation (Å)	MoK α	MoK α
	($\lambda = 0.71073$)	($\lambda = 0.71073$)
a (Å)	18.5689(4)	12.9173(3)
b (Å)	15.4573(4)	13.0433(2)
c (Å)	18.2748(5)	19.2711(3)
α (°)	90	107.7810(10)
β (°)	100.328(2)	97.242(2)
γ (°)	90	97.459(2)
Volume/(Å³)	5160.3(2)	3018.03(10)
Z	4	2
Temperature (K)	293(2)	293(2)
Independent reflections	10813	12603
Data/restrains/parameters	10813/2/541	12603/0/779
D_{calcd} [g cm⁻³]	1.018	1.284
F(000)	1656.0	1236.0
R factor [I > 2σ(I)]	R ₁ = 0.0606, wR ₂ = 0.1871	R ₁ = 0.0713, wR ₂ = 0.1667
R factor (all data)	R ₁ = 0.0905 wR ₂ = 0.2030	R ₁ = 0.1398 wR ₂ = 0.2108
GoF	1.100	1.050
CCDC number	2099945	2070350

Table S1 (b). Crystallographic data and structure refinement for Trip-COOH and Trip(CH₃)-COOH.

Sample code	Trip-COOH (8c)	Trip(CH ₃)-COOH (8d)
Crystal system	triclinic	monoclinic
Space group	P-1	C 2/c
Chemical formula	C ₄₄ H ₄₂ O ₁₁	C ₄₂ H ₄₀ O ₆
Formula weight	746.77	640.78
Radiation (Å)	MoK α	MoK α
	($\lambda = 0.71073$)	($\lambda = 0.71073$)
a (Å)	8.37800(1)	32.9760(19)
b (Å)	13.2003(3)	7.9644(3)
c (Å)	17.8121(5)	31.495(2)
α (°)	72.054 (2)	90
β (°)	84.683(2)	112.675(7)
γ (°)	83.825(2)	90
Volume/(Å³)	1859.47(7)	7632.3(8)
Z	2	8
Temperature (K)	293(2)	293(2)
Independent reflections	6553	6726
Data/restrains/parameters	6553/2/504	6726/0/489
D_{calcd} [g cm⁻³]	1.334	1.115
F(000)	788.0	2720.0
R factor [I > 2 σ(I)]	R ₁ = 0.0459	R ₁ = 0.0957
R factor (all data)	wR ₂ = 0.1207	wR ₂ = 0.2795
	R ₁ = 0.0583	R ₁ = 0.1558
	wR ₂ = 0.1307	wR ₂ = 0.3168
GoF	1.069	1.065
CCDC number	2070384	1951204

Section S7. Screening conditions for diacid monomer (PenTrip-COOH)

Table S2. Synthetic conditions that were screened for synthesizing PenTrip-COOH.

Entry	Reactant (6.98 g)	Base (4 eq.)	Solvent	Temp. (°C)	Reaction Time	Yield of PenTrip-CO ₂ H (%)
1	PenTrip-CN	KOH	EtOH+H ₂ O (1/1 by vol.)	90	48 h, reflux	2
2	PenTrip-CN	KOH	EtOH+MeOH+H ₂ O (1/1/1 by vol.)	85	72 h, reflux	0
3	PenTrip-CN	KOH	MeOH+H ₂ O (1/1 by vol.)	65	48 h, reflux	1
4	PenTrip-CN	NaOH	EtOH+H ₂ O (1/1 by vol.)	90	48 h, reflux	0
5	PenTrip-CN	NaOH	EtOH+MeOH+H ₂ O (1/1/1 by vol.)	85	24 h, reflux	0
6	PenTrip-CN	tBuOK	EtOH+H ₂ O (1/1 by vol.)	95	48 h, reflux	5
7	PenTrip-CN	tBuOK	EtOH+MeOH+H ₂ O (1/1/1 by vol.)	85	24 h, reflux	10
8	PenTrip-CN	KOH	Triethylene glycol	200	48 h, reflux	89
9	PenTrip-CN	NaOH	Triethylene glycol	200	48 h, reflux	65

Section S8. Screening conditions for polymer PenTrip-PyPBI

Table S3. Screening of conditions for PenTrip-PyPBI synthesis.

Entry	Reactant 1 (5 mmol)	Reactant 2 (5 mmol)	Solvent	Temp. (°C)	Time and atmosphere	Observation and yield of PenTrip-PyPBI
1	PenTrip-CO ₂ H	PyTAB	PPA+P ₂ O ₅ ^a	220	24 h, N ₂	0 (%)
2	PenTrip-CO ₂ H	PyTAB	PPA+NMP	190	24 h, N ₂	0 (%)
3	PenTrip-CO ₂ H	PyTAB	PPMA	160	8 h, N ₂	10 (%)
4	PenTrip-CO ₂ H	PyTAB	PPMA+P ₂ O ₅ ^a	160	16 h, N ₂	8 (%)
5	PenTrip-CO ₂ H	PyTAB	PPMA+NMP ^b +P ₂ O ₅	150	16 h, N ₂	15 (%)
6	PenTrip-CO ₂ H	PyTAB	CH ₃ SO ₃ H	140	16 h, N ₂	0 (%)
7	PenTrip-CO ₂ H	PyTAB	CF ₃ SO ₃ H+P ₂ O ₅	140	2.5 h N ₂	Viscous but not soluble
8	PenTrip-CO ₂ H	PyTAB	PPMA+ CF ₃ SO ₃ H	140	3 h, N ₂	Viscous, easy to stir, 80 (%)
9	PenTrip-CO ₂ H	PyTAB	PPMA+ CF ₃ SO ₃ H+ P ₂ O ₅ ^c	140	3 h, N ₂	Viscous, easy to stir, 98 (%)

^a The content of added P₂O₅ was calculated for a total PPA concentration of 128 wt%.

^b The added P₂O₅ content is equal to 5 wt% of PPA.

^c The added content P₂O₅ content is equal to 5 wt% of PPA.

Section 9. Viscosity, molecular weight, solubility and XPS results of 3D iptycene-based PyPBIs

Table S4. Inherent viscosity, viscosity average molecular weight (\overline{M}_v) and solubility results of the iptycene-based PyPBI polymers.

Sample code	I.V (dL/g)	\overline{M}_v^a (kDa)	DMSO	DMAc	MSA	DMF	FA
Trip-PyPBI	1.32	9.4	++	++	++	++	++
Trip(CH₃)-PyPBI	2.00	9.7	++	++	++	++	++
PenTrip-PyPBI	1.77	9.3	++	++	++	++	++
PenTrip(CH₃)-PyPBI	2.11	12.9	++	++	++	++	++

++ completely Soluble at room temperature up to 2 wt%.

^a \overline{M}_v obtained from Mark–Houwink–Sakurada equation $[\eta] = K\overline{M}_v^a$ where $K = 5.2 \times 10^{-5}$ dL/g

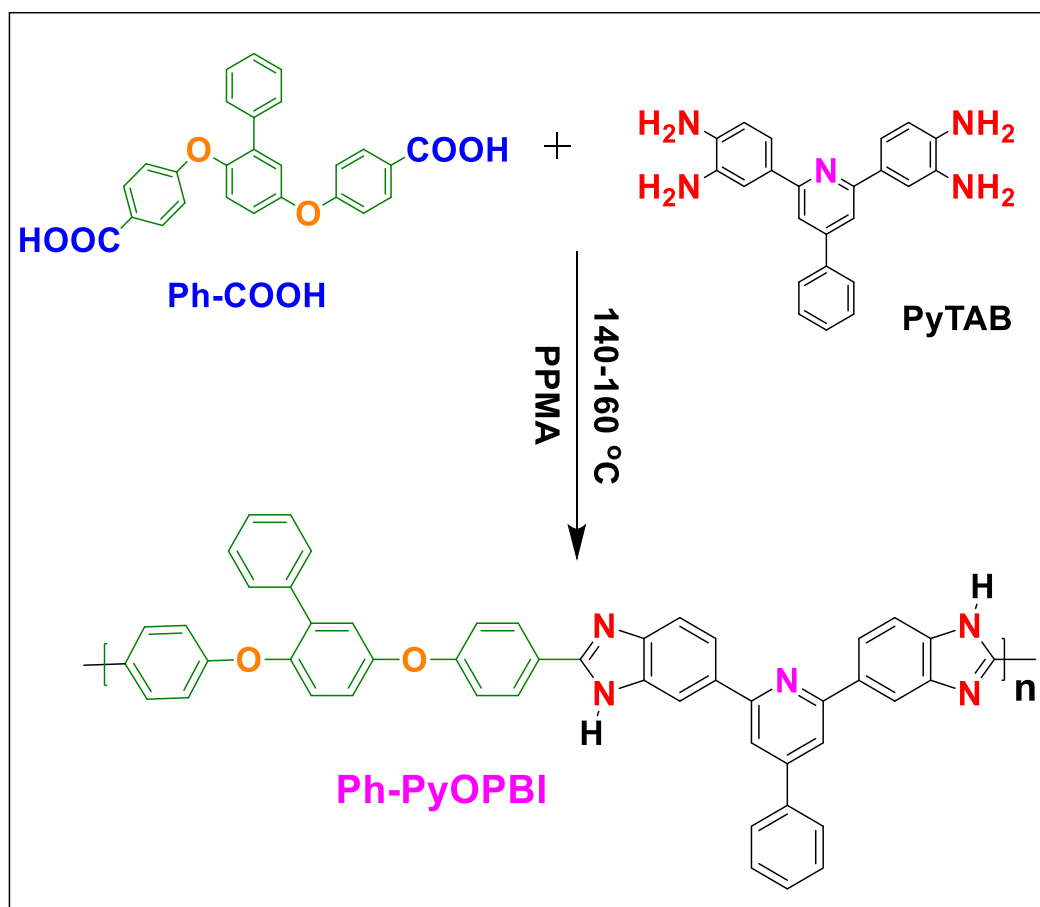
and $a = 0.92$ and $[\eta] = \frac{\eta_{sp} + 3 \ln \eta_{rel}}{4C}$ where $\eta_{sp} = 1 - \eta_{rel}$ and $\eta_{rel} = t/t_o$ where t and t_o are the time

flow for the polymer solution and solvent, respectively.⁶

Table S5. Atomic elemental contents (C, O and N) of 3D iptycene-based PyPBIs calculated by XPS.

Samples	C 1s (atomic %)	N 1s (atomic %)	O 1s (atomic %)
Trip-PyPBI	83.82	4.18	11.99
Trip(CH ₃)-PyPBI	88.58	2.91	8.51
PenTrip-PyPBI	89.18	2.29	8.49
PenTrip(CH ₃)-PyPBI	89.75	1.91	8.34

Section 10. Synthetic route of Ph-PyOPBI



Scheme S1. Synthesis of Ph-PyOPBI polymer.

Section S11. NMR (^1H & ^{13}C) and FT-IR spectra of intermediates and diacid monomers

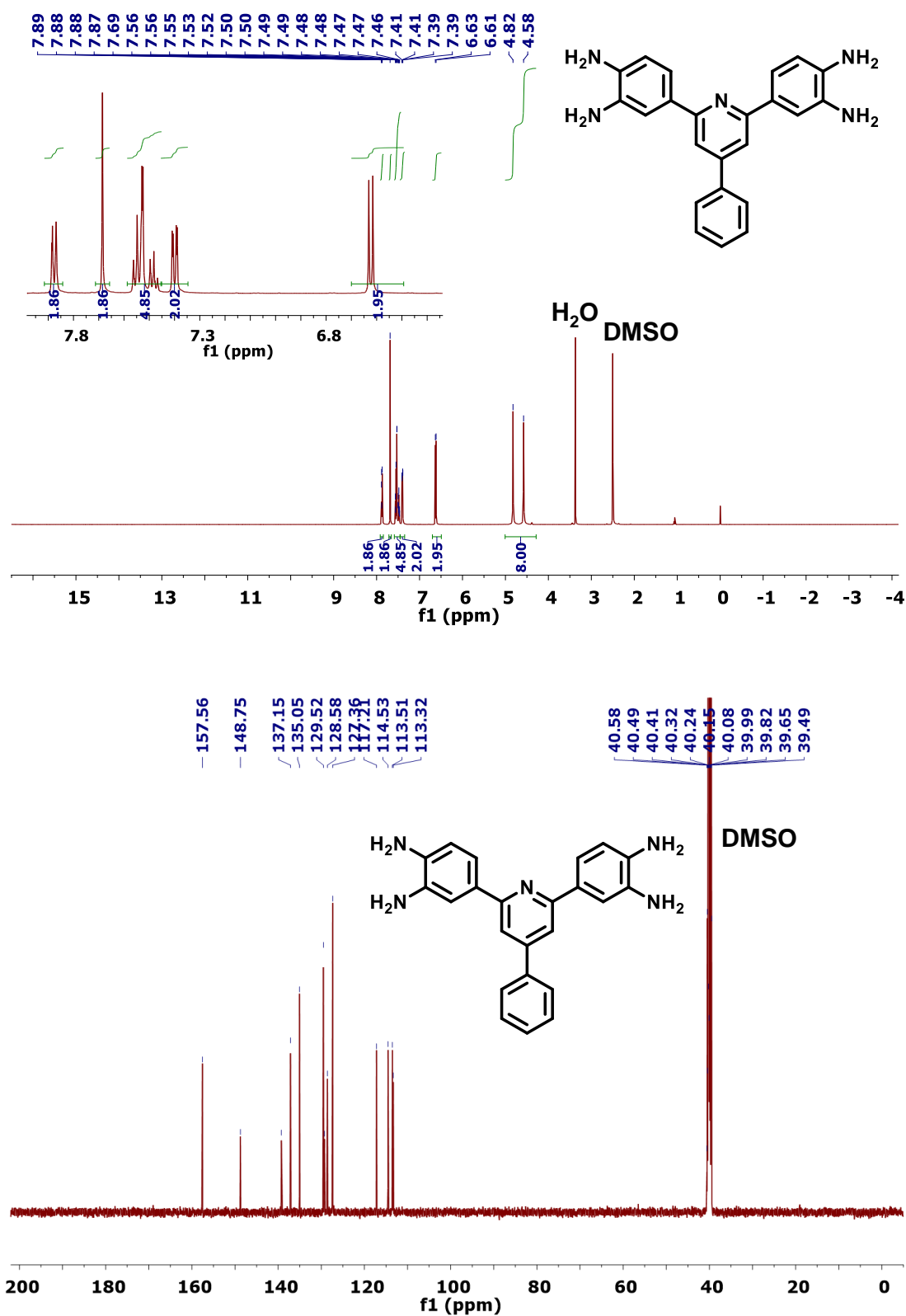


Figure S1. ^1H NMR and ^{13}C NMR spectra of PyTAB. DMSO- d_6 is used as NMR solvent.

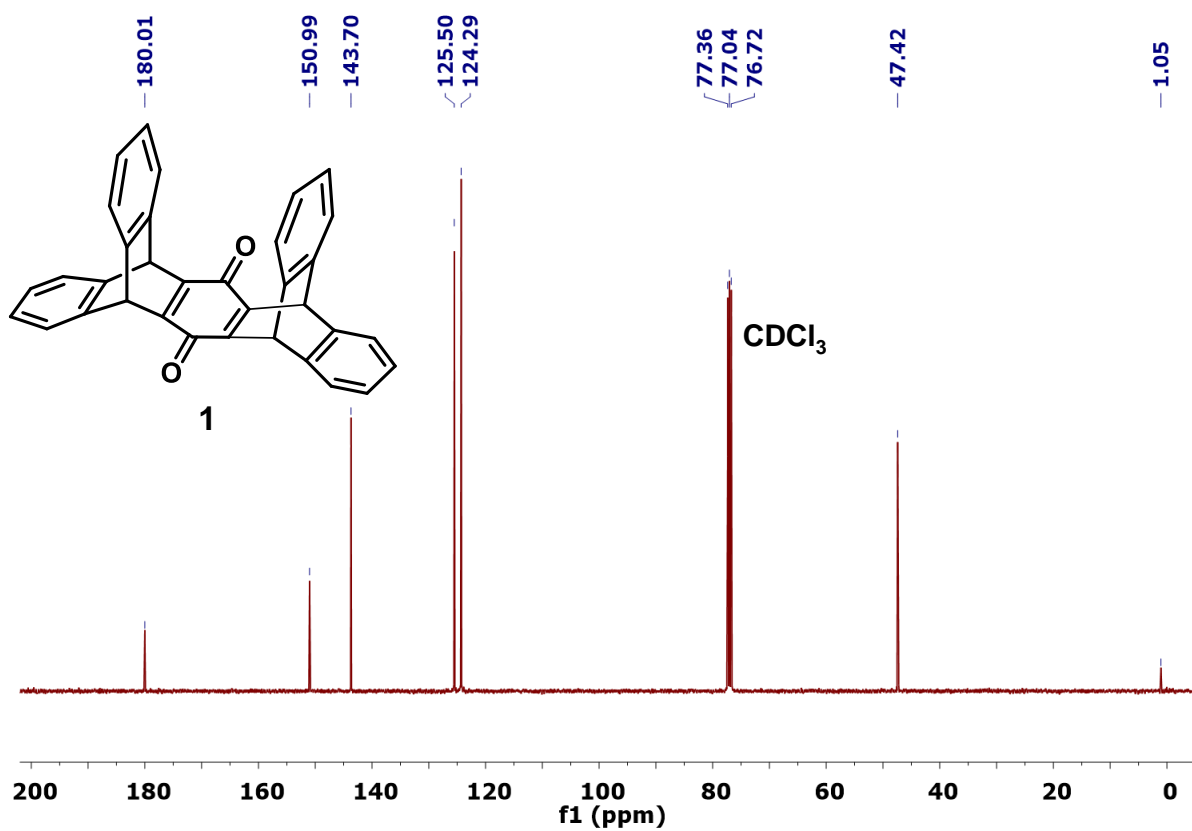
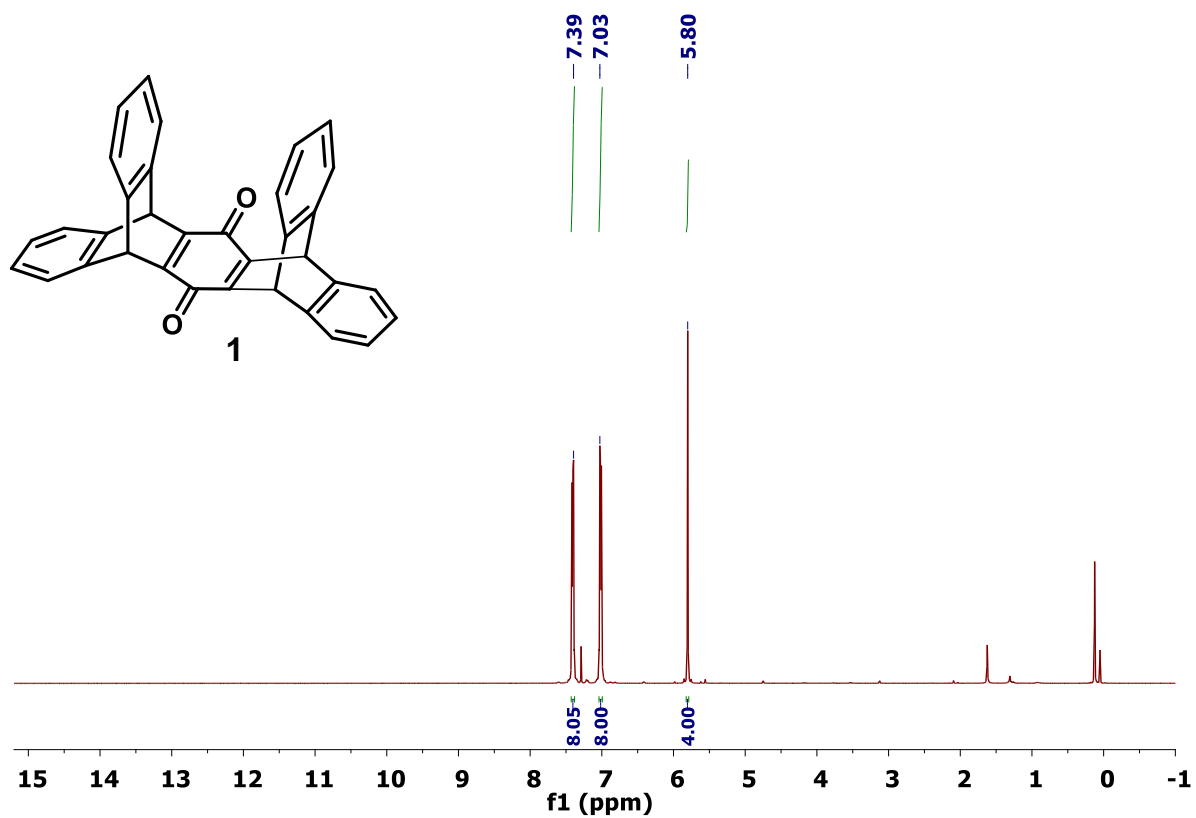


Figure S2. ¹H and ¹³C NMR spectra of pentiptycene quinone (**1**). NMR solvent: CDCl₃

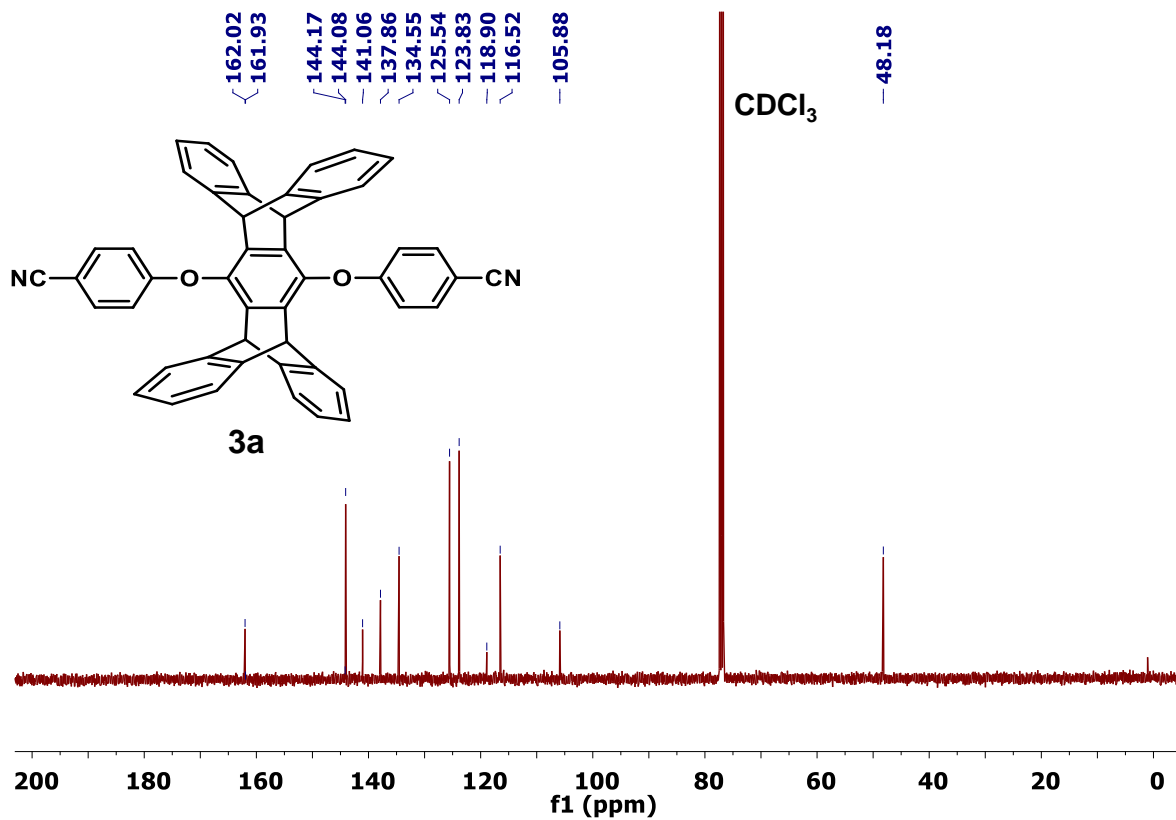
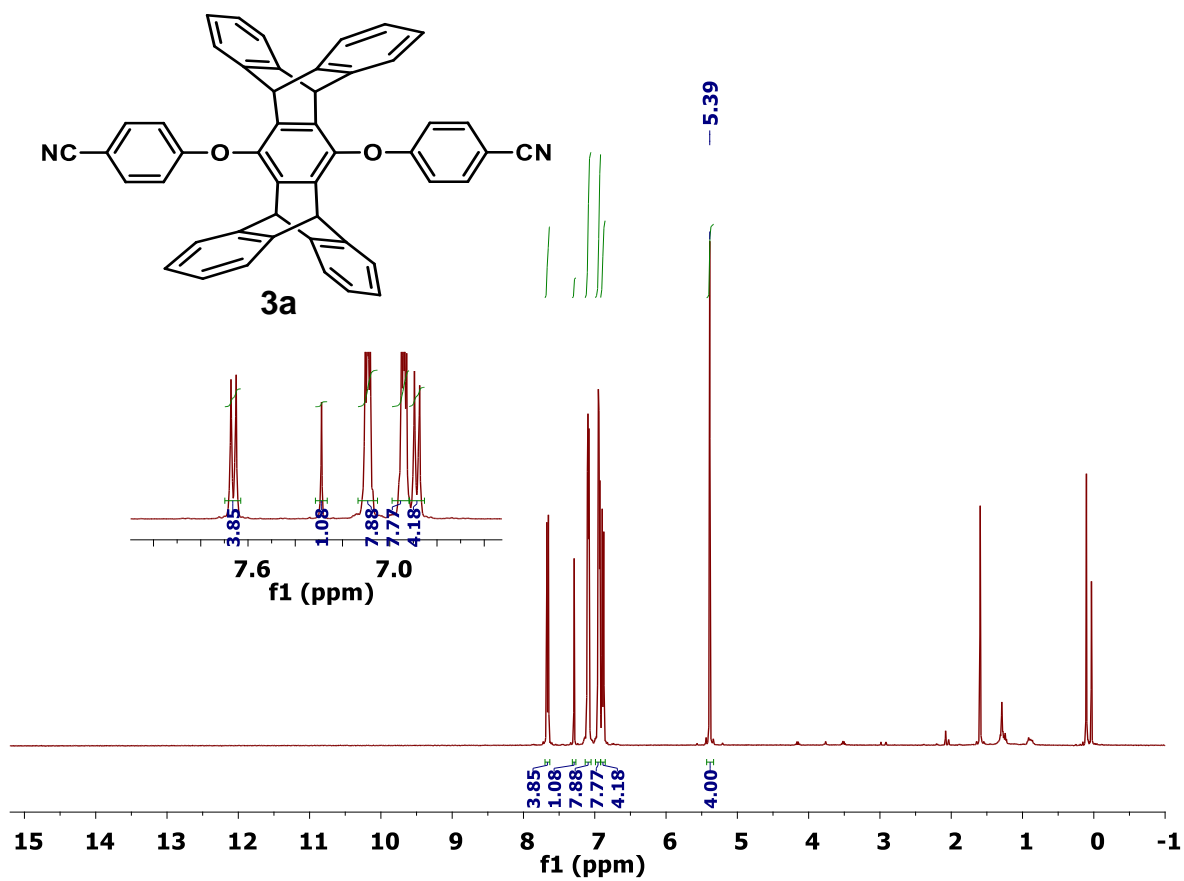


Figure S4. ^1H and ^{13}C NMR spectra of PenTrip-CN (3a). NMR solvent: CDCl₃.

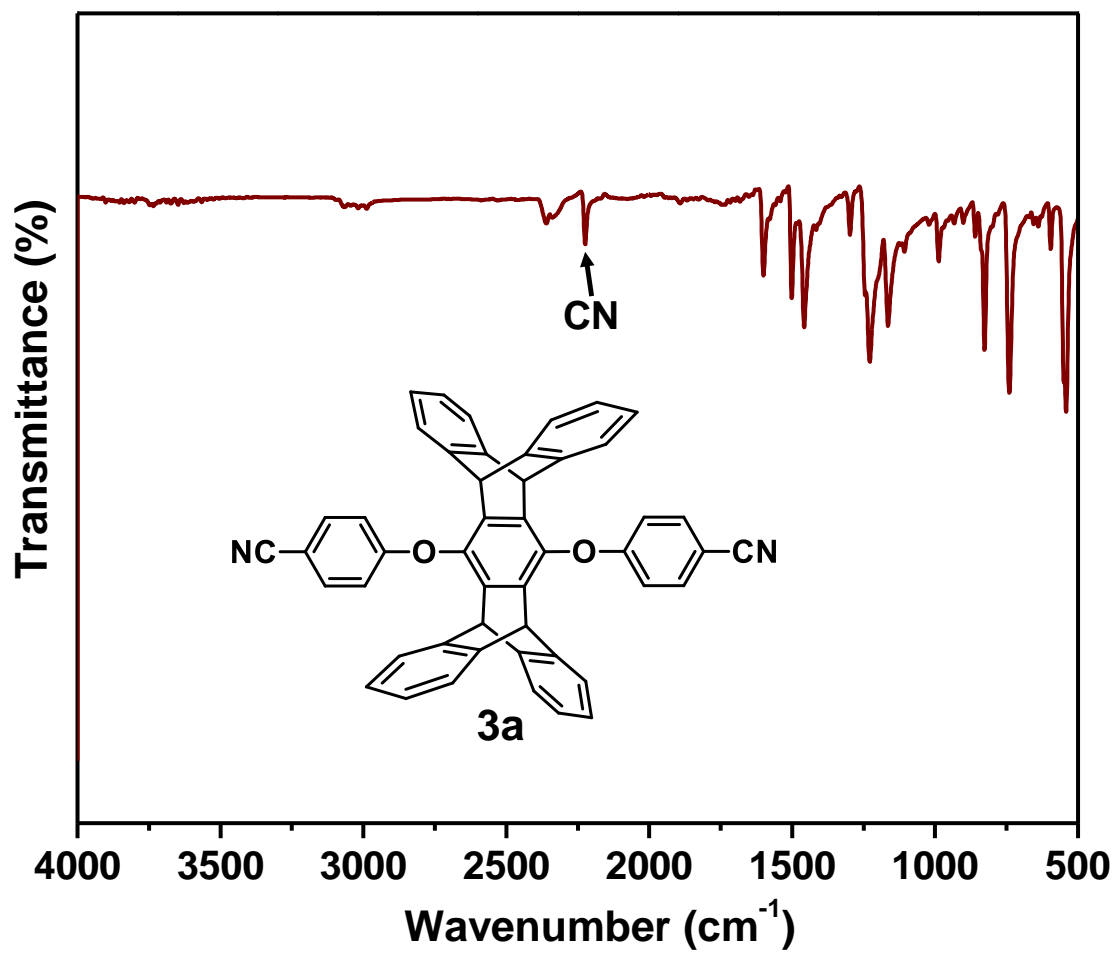


Figure S5. FTIR spectra of PenTrip-CN (3a).

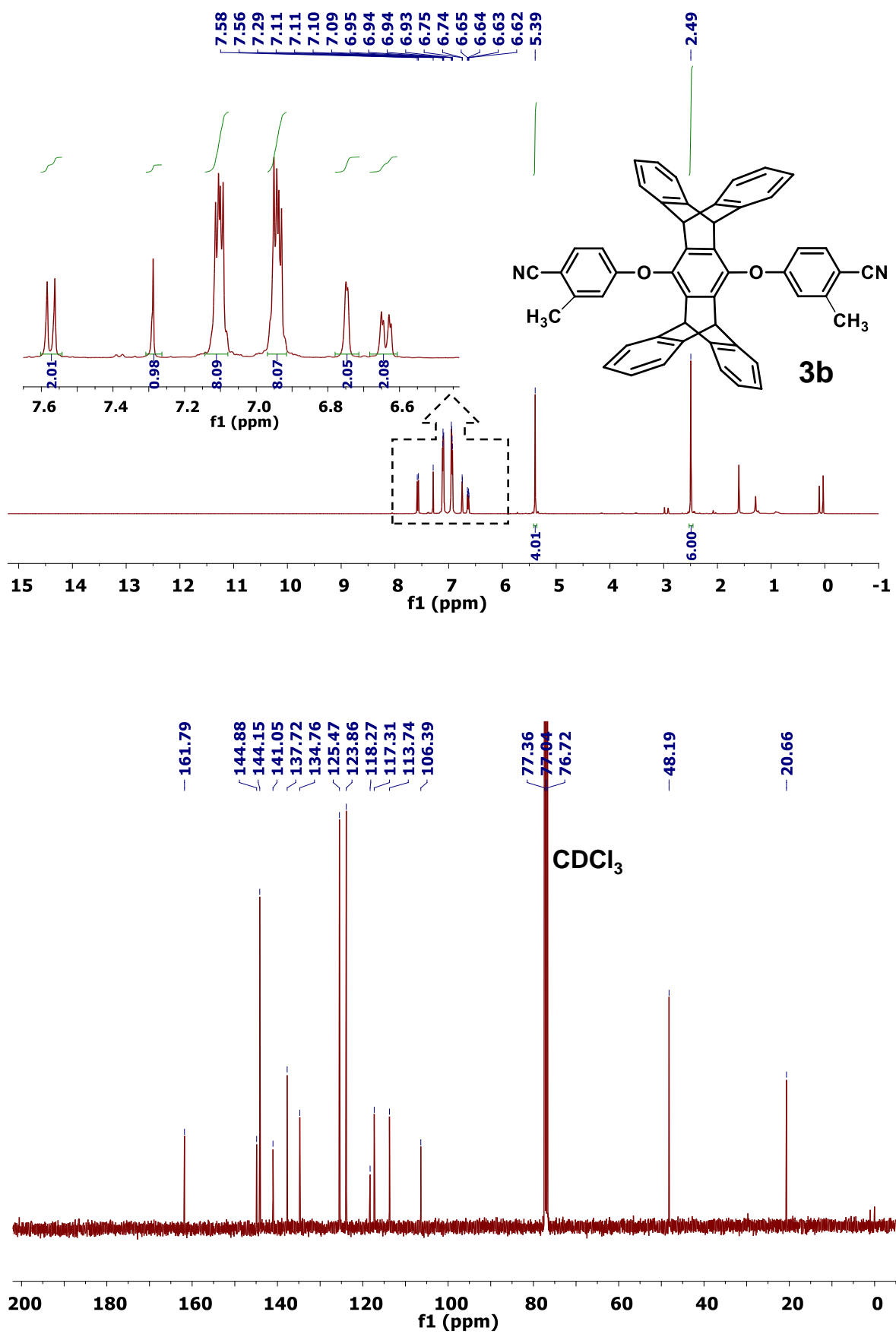


Figure S6. ¹H and ¹³C NMR spectra of PenTrip(CH₃)-CN (**3b**). NMR solvent: CDCl₃.

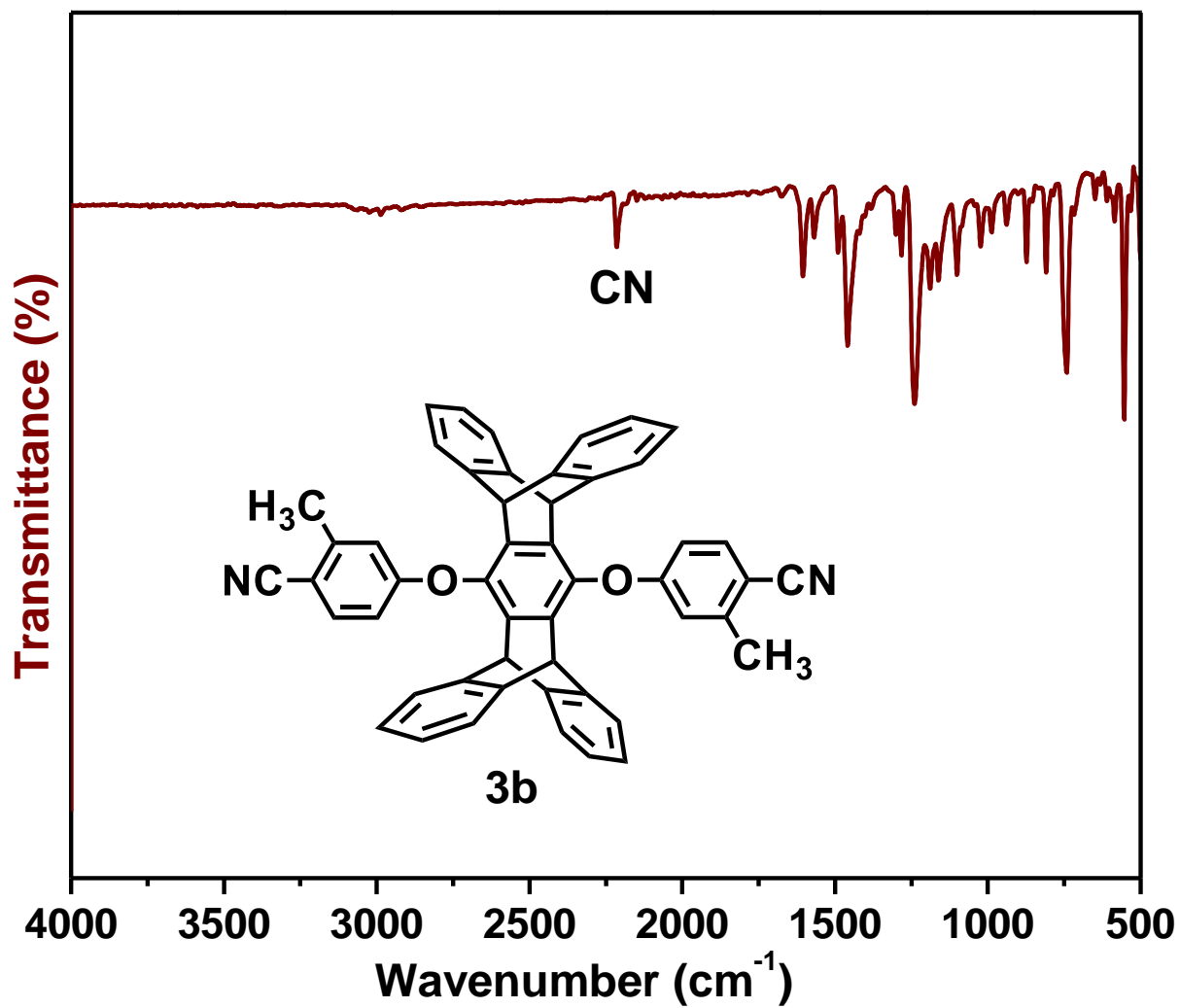


Figure S7. FTIR spectra of PenTrip(CH₃)-CN (3b).

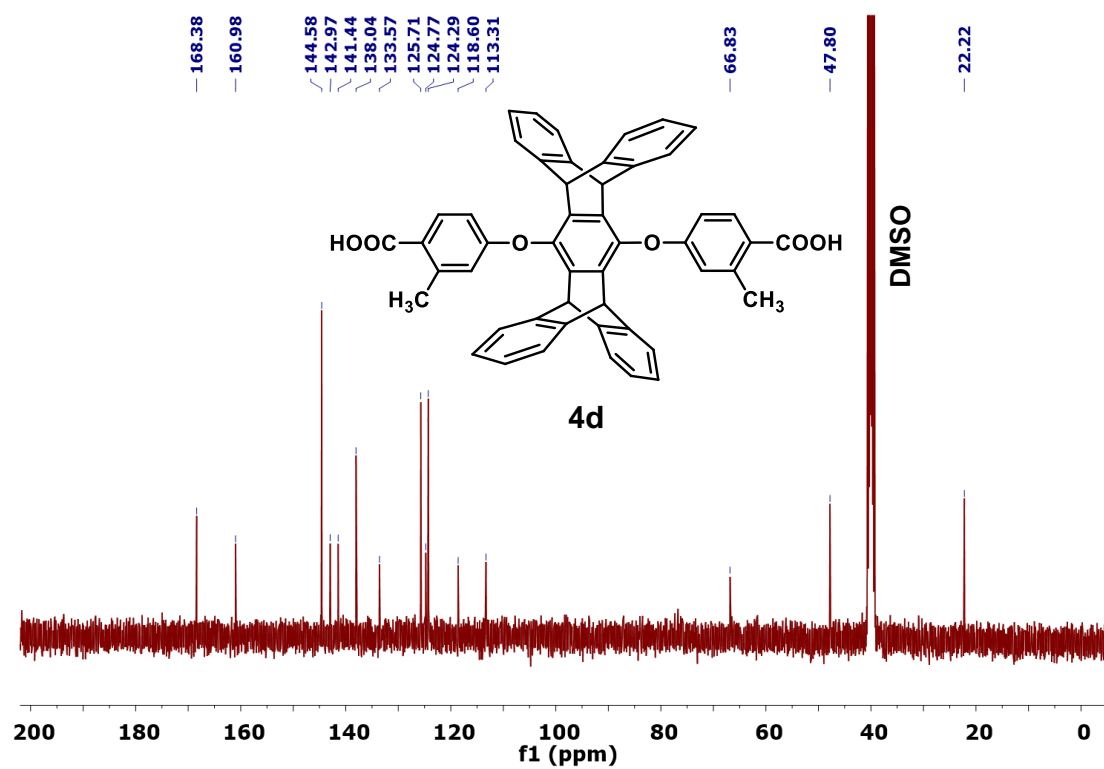
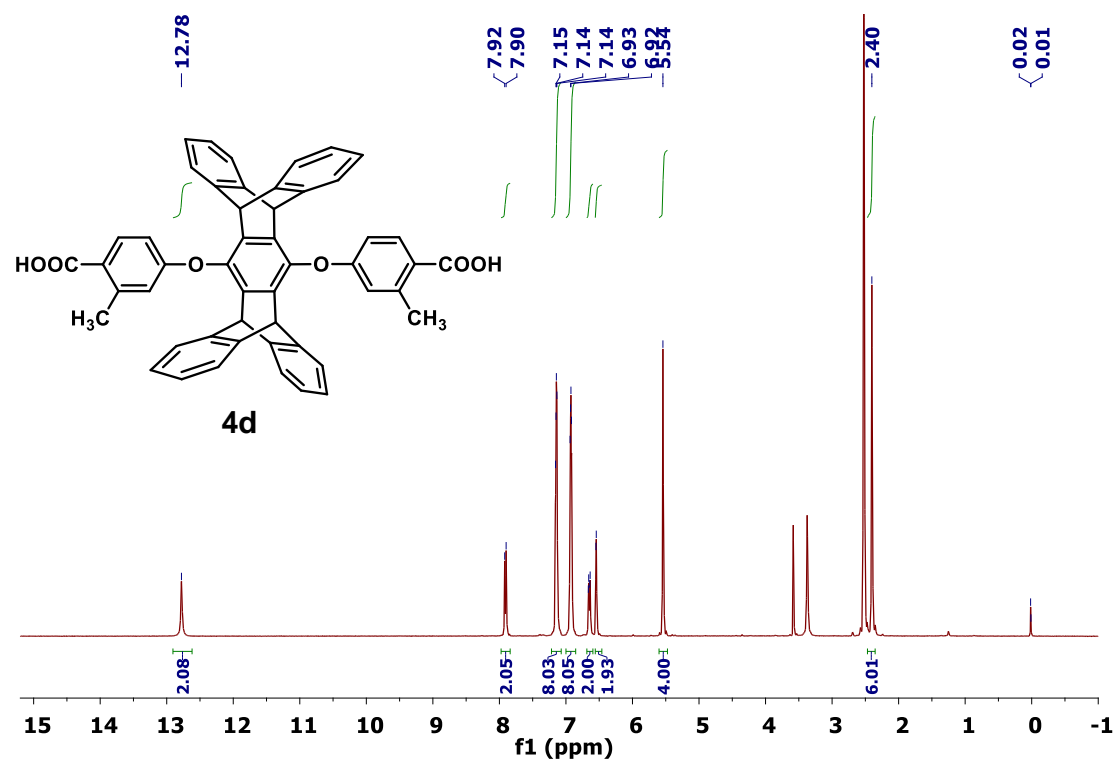


Figure S9. ¹H and ¹³C NMR spectra of PenTrip(CH₃)-COOH (**4d**). NMR solvent: DMSO-*d*₆.

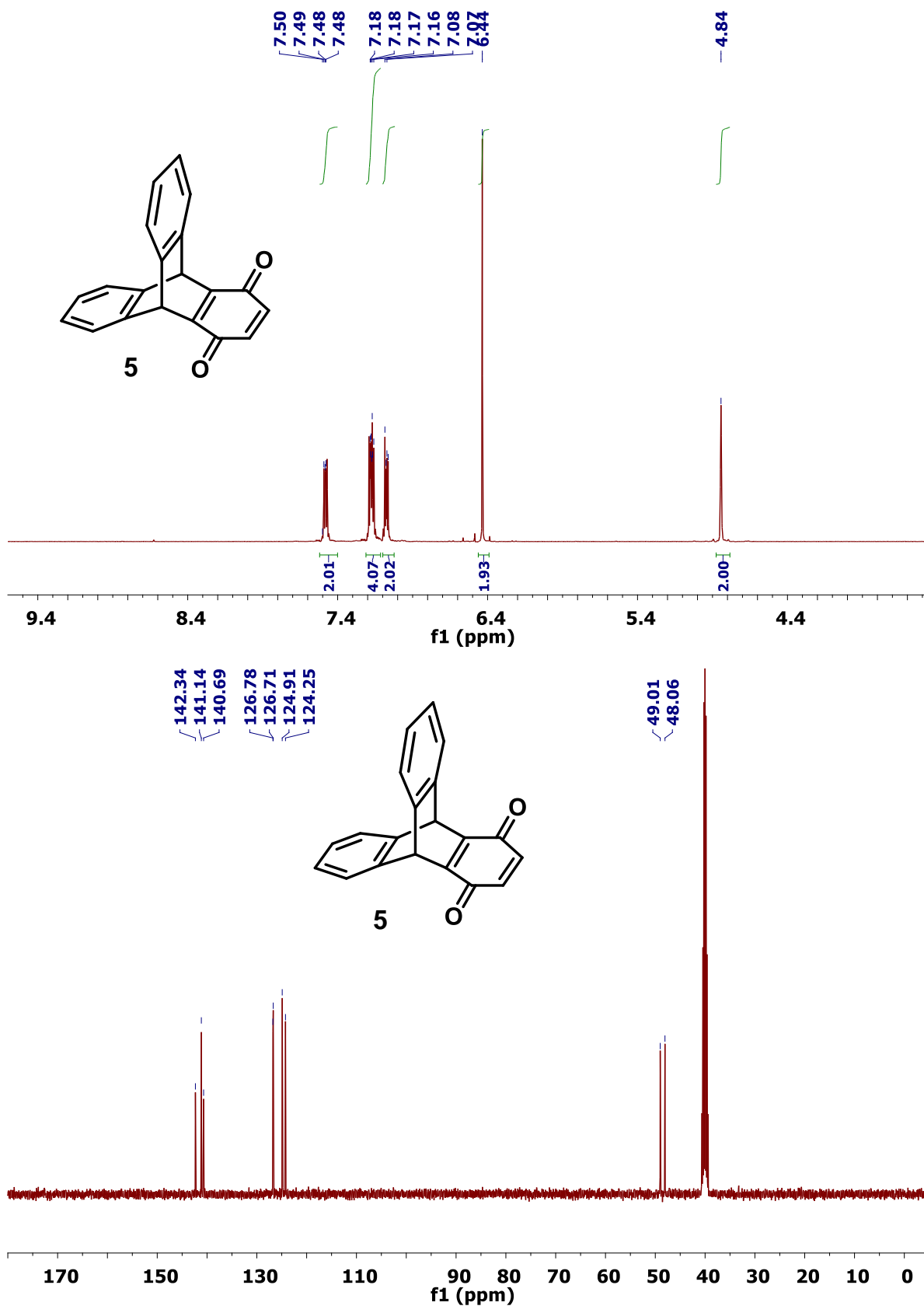


Figure S10. ¹H and ¹³C NMR spectra of triptycene quinone (**5**). NMR solvent: DMSO-*d*₆.

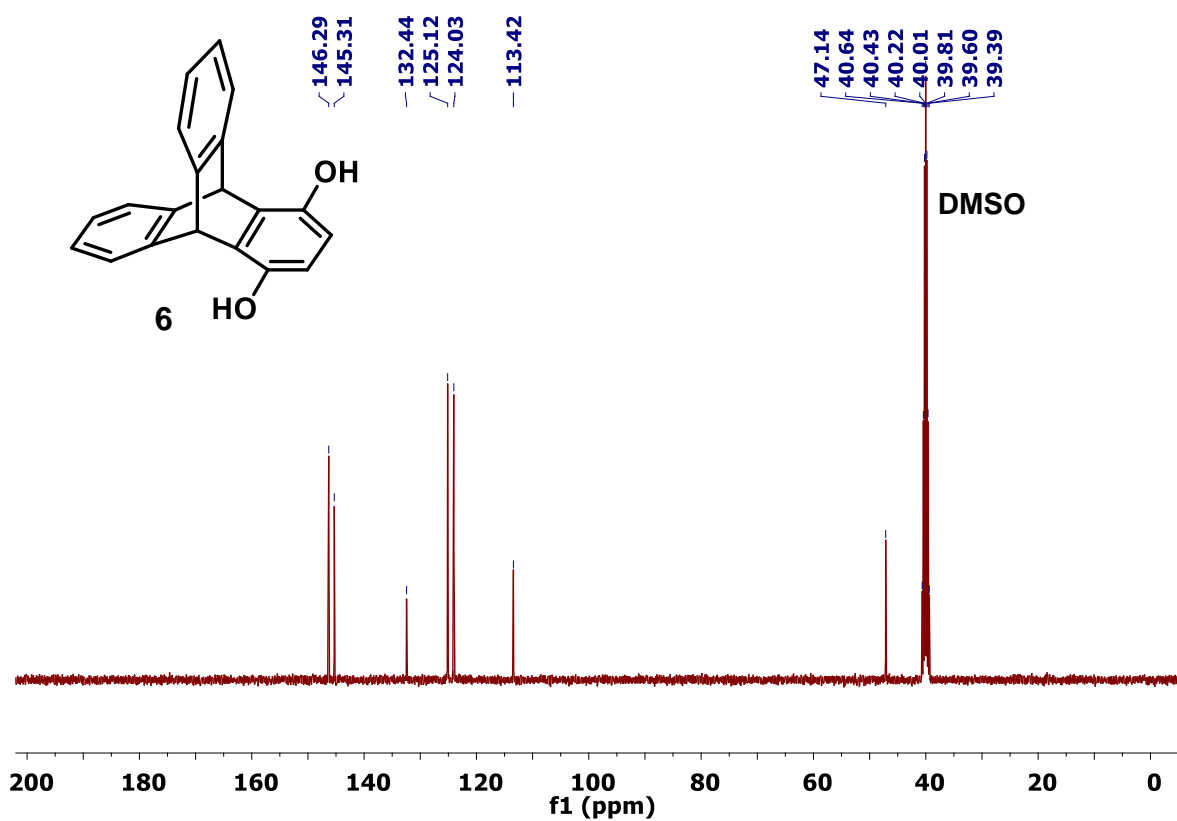
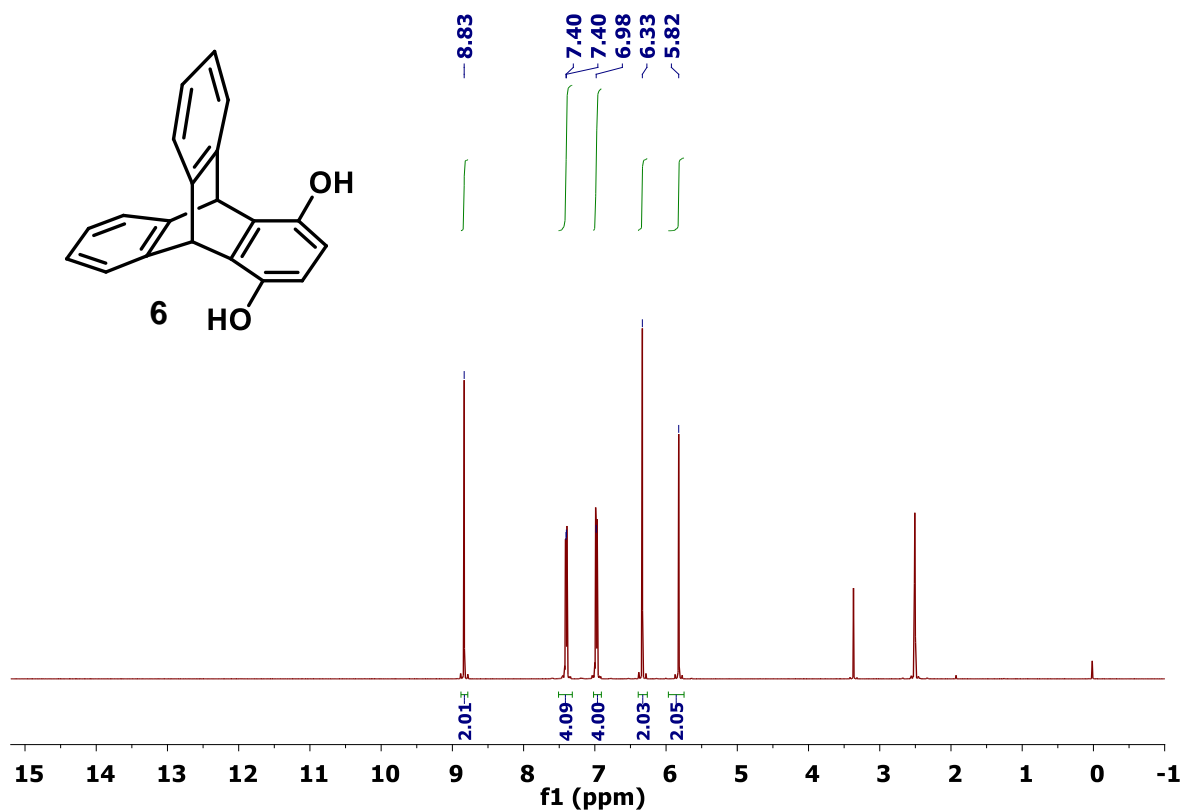


Figure S11. ¹H and ¹³C NMR spectra of triptycene hydroquinone (**6**). NMR solvent: DMSO-*d*₆.

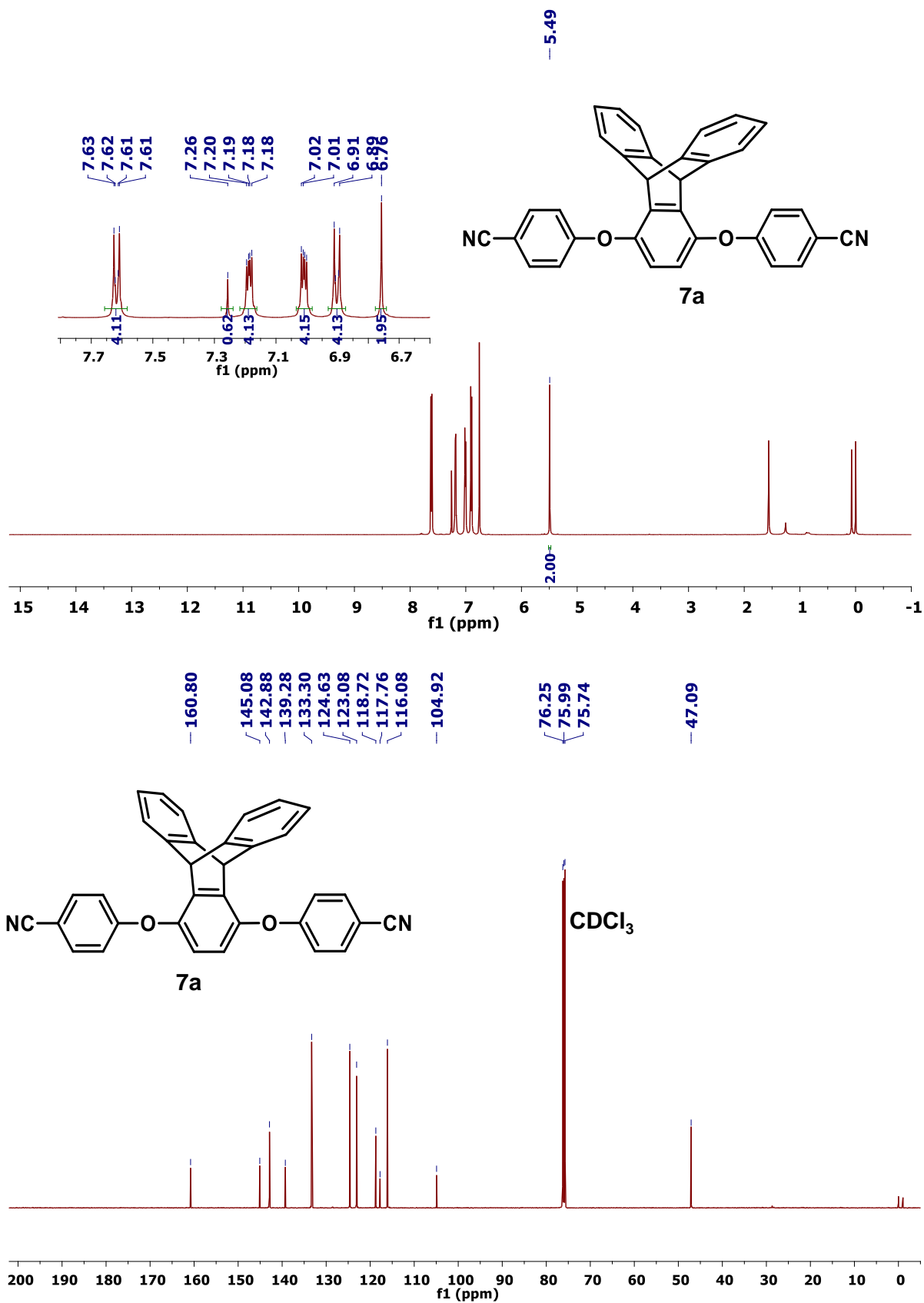


Figure S12. ¹H and ¹³C NMR spectra of Trip-CN (7a). NMR solvent: CDCl₃.

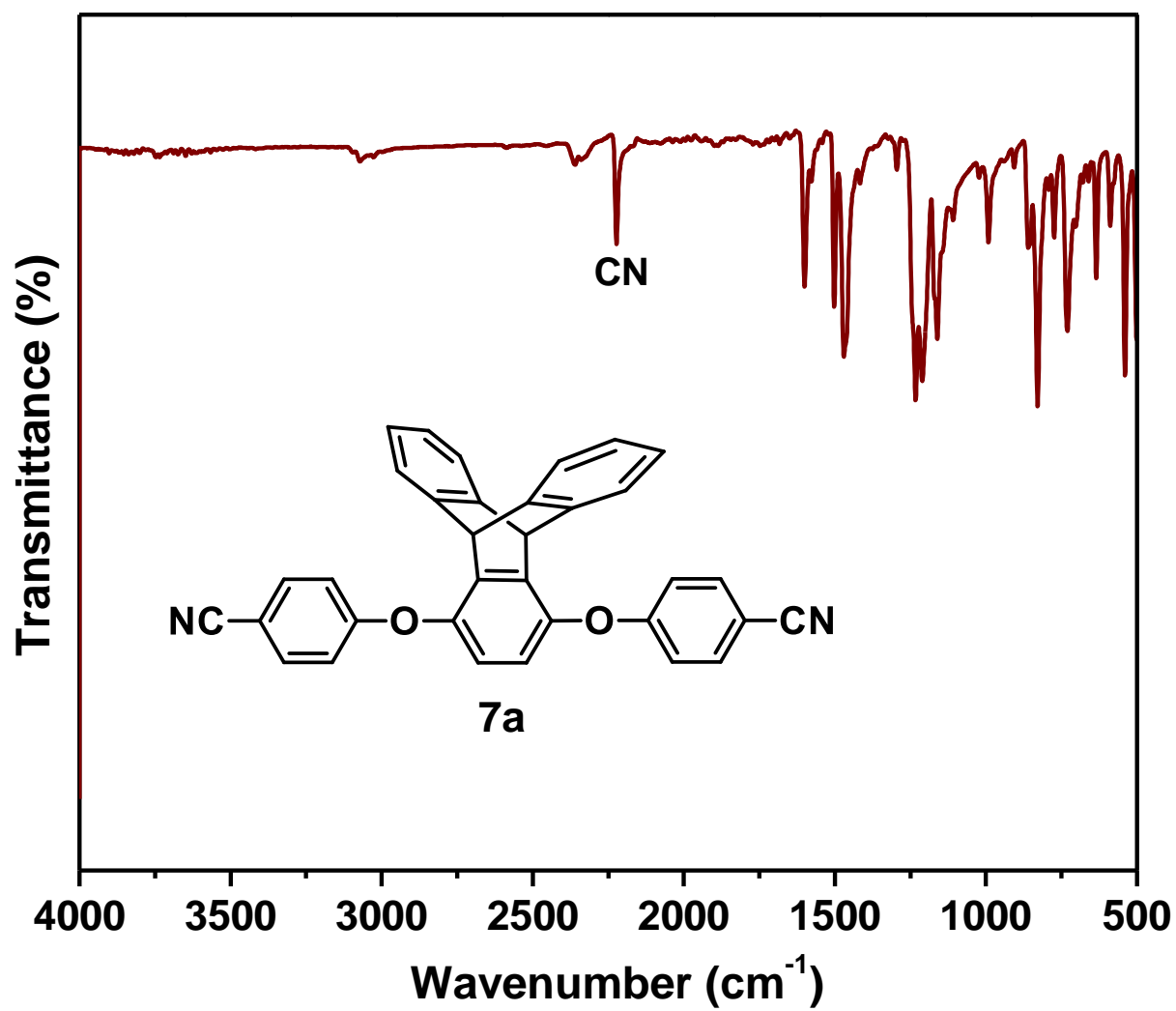


Figure S13. FT-IR spectra of Trip-CN compound (7a).

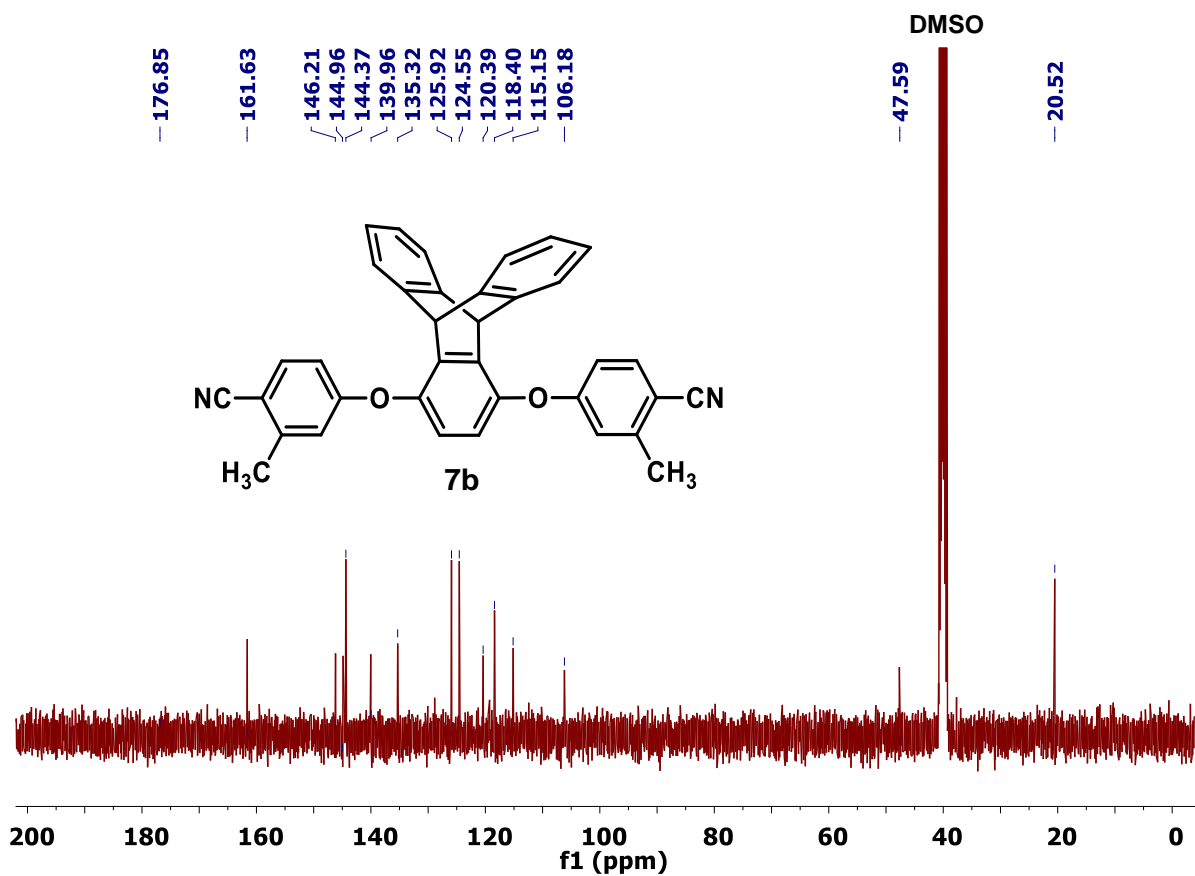
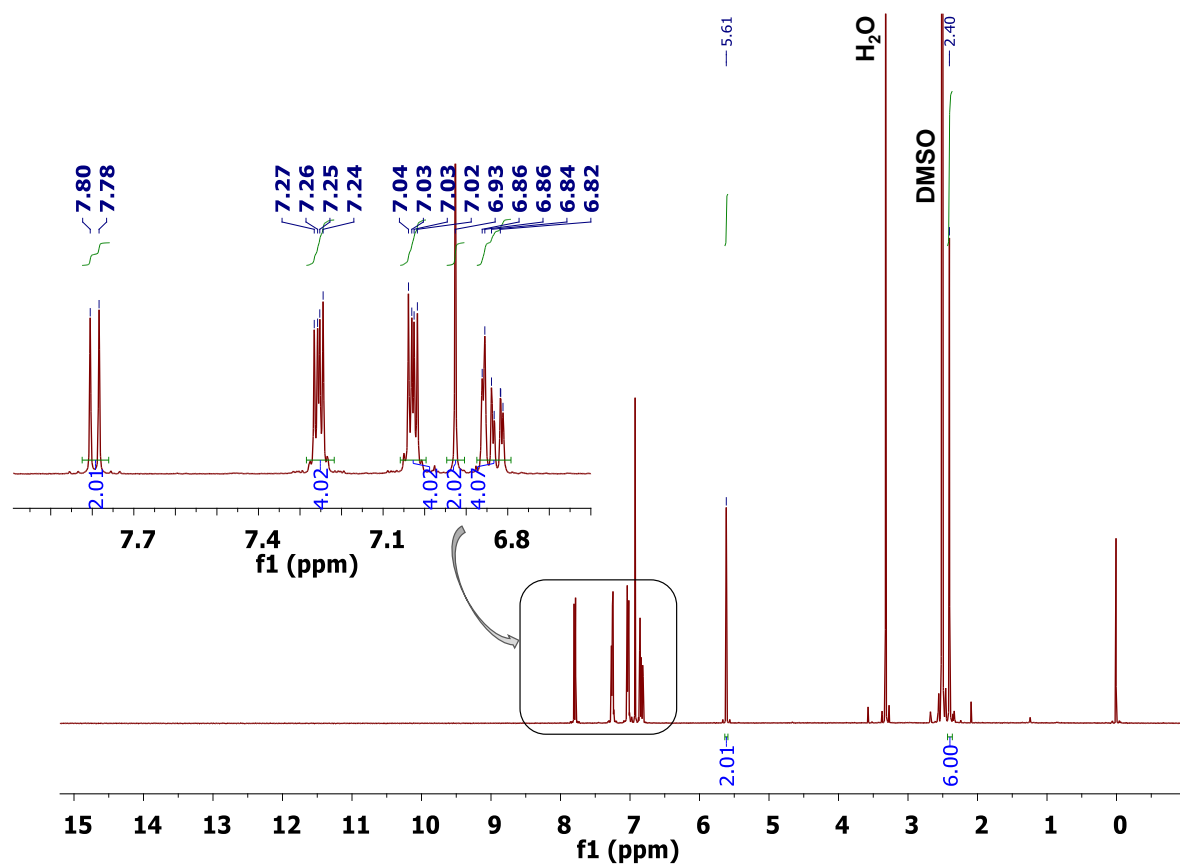


Figure S14. ¹H and ¹³C NMR spectra of Trip(CH₃)-CN (**7b**). NMR solvent: DMSO-*d*₆.

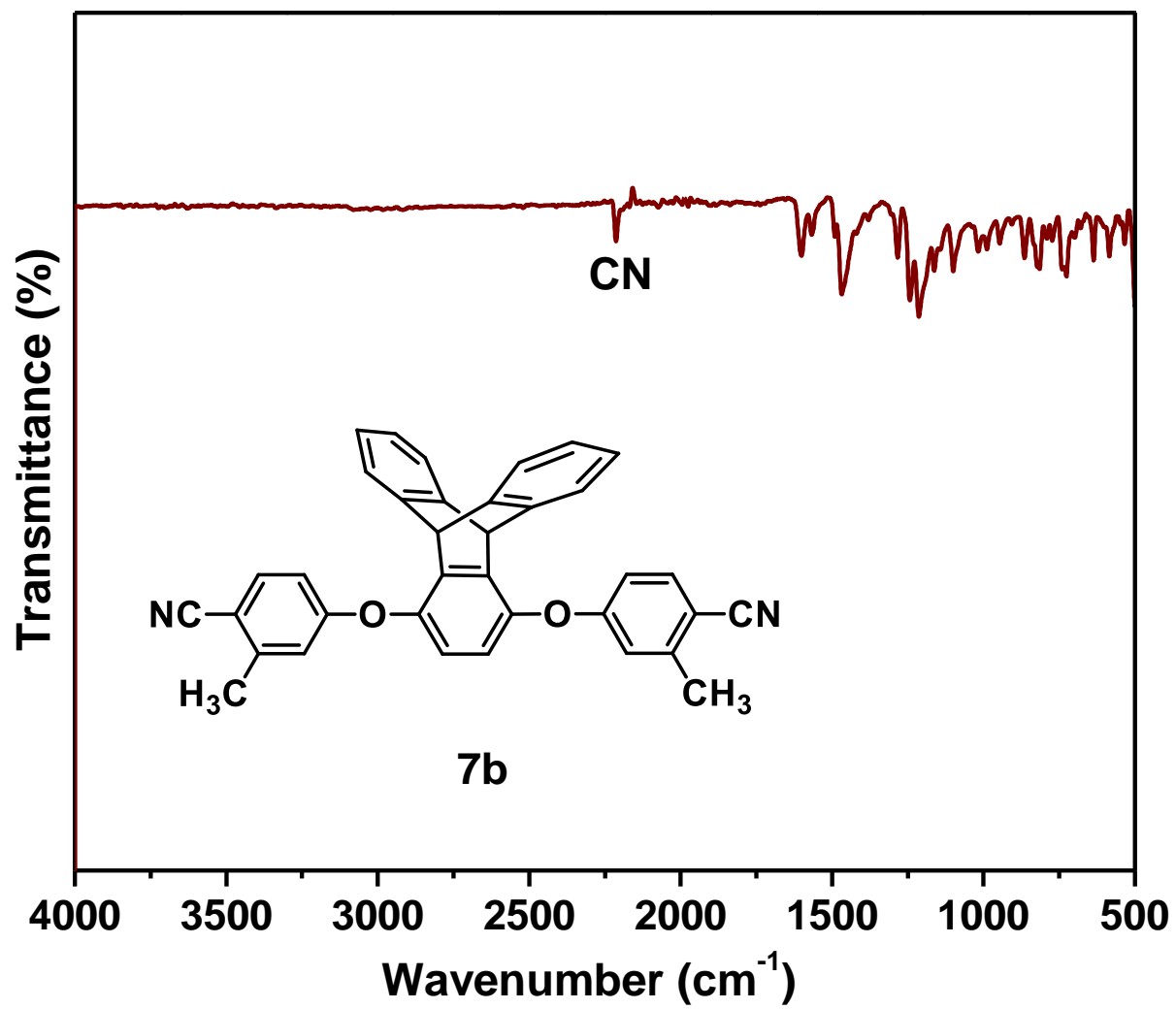


Figure S15. FT-IR spectra of Trip(CH₃)-CN compound (**7b**).

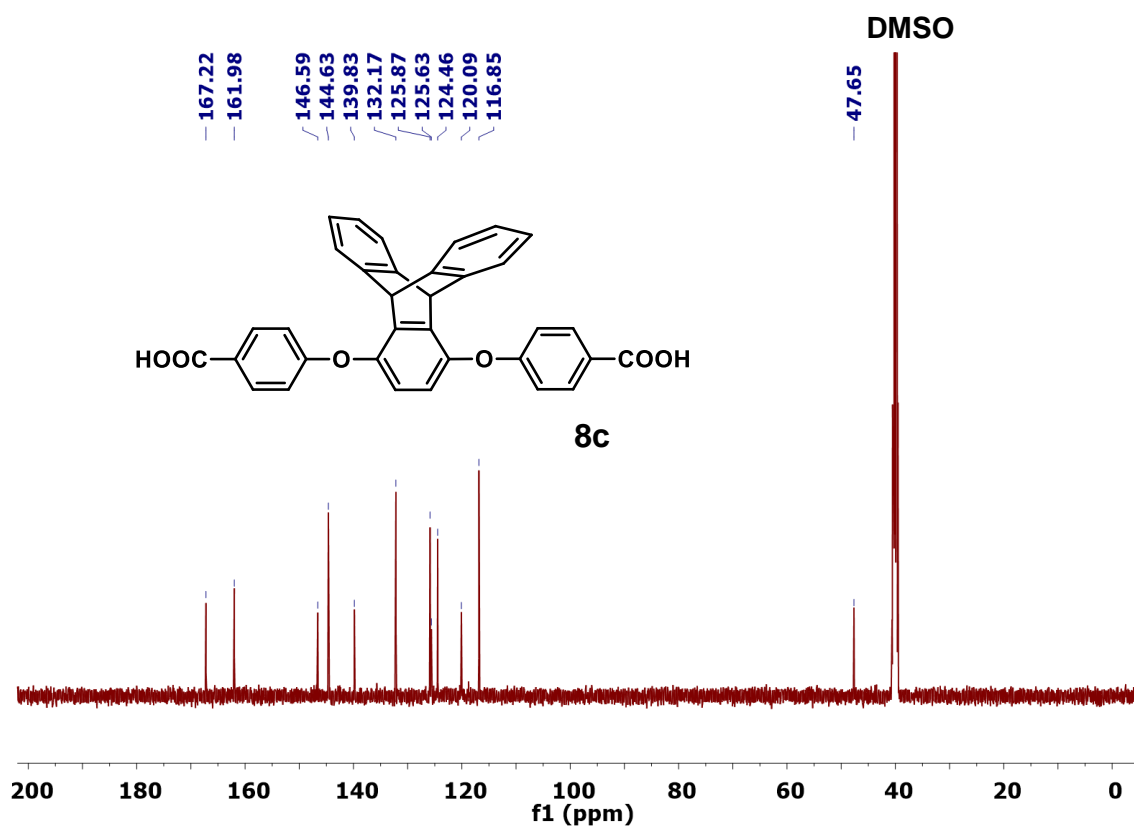
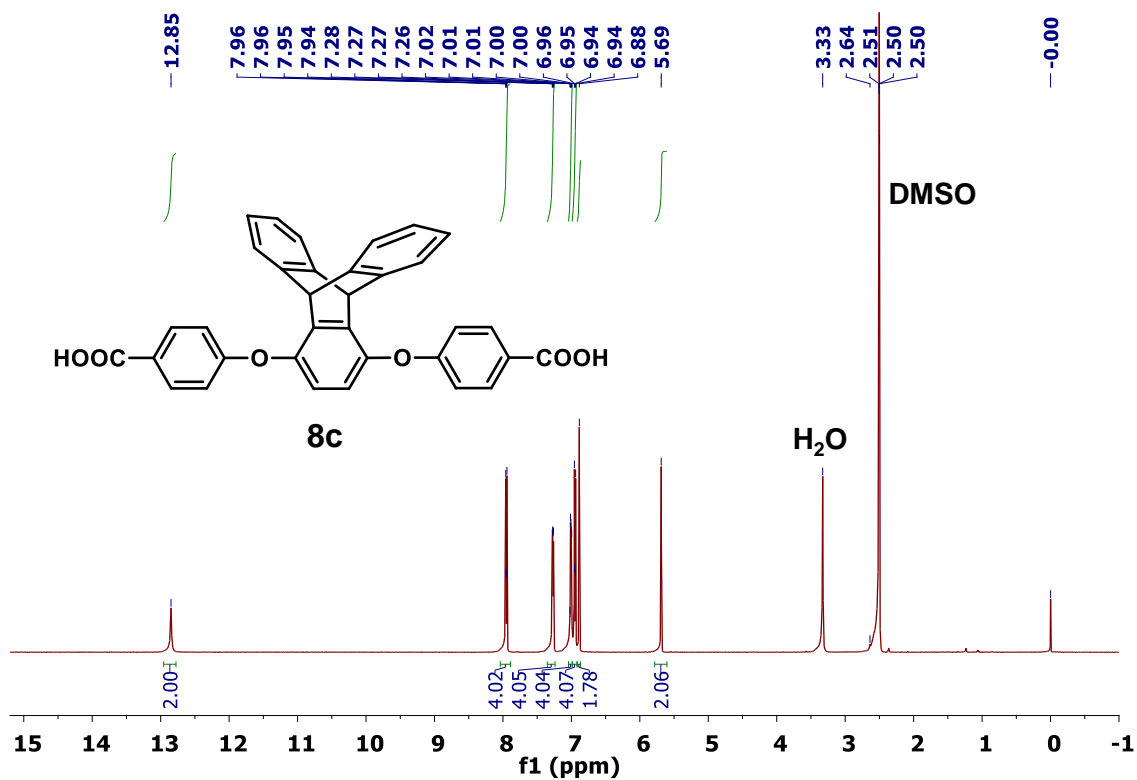


Figure S16. ¹H and ¹³C NMR spectra of Trip-COOH (**8c**). NMR solvent: DMSO-*d*₆.

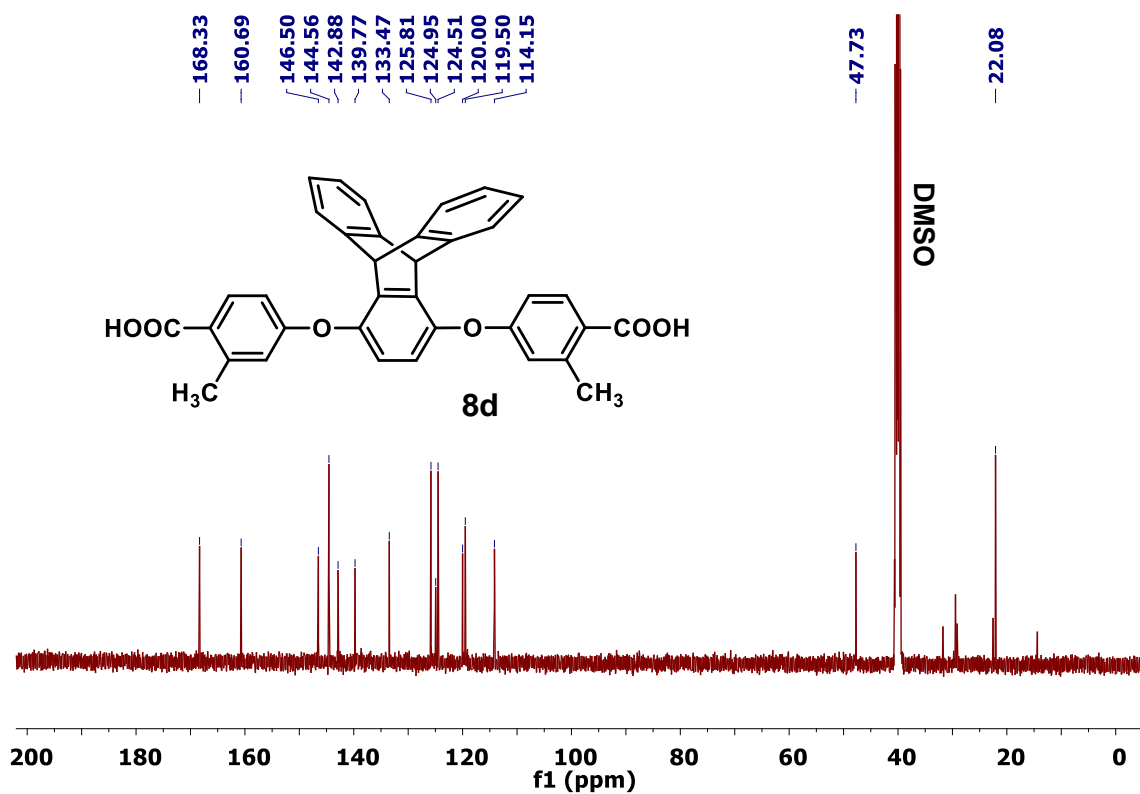
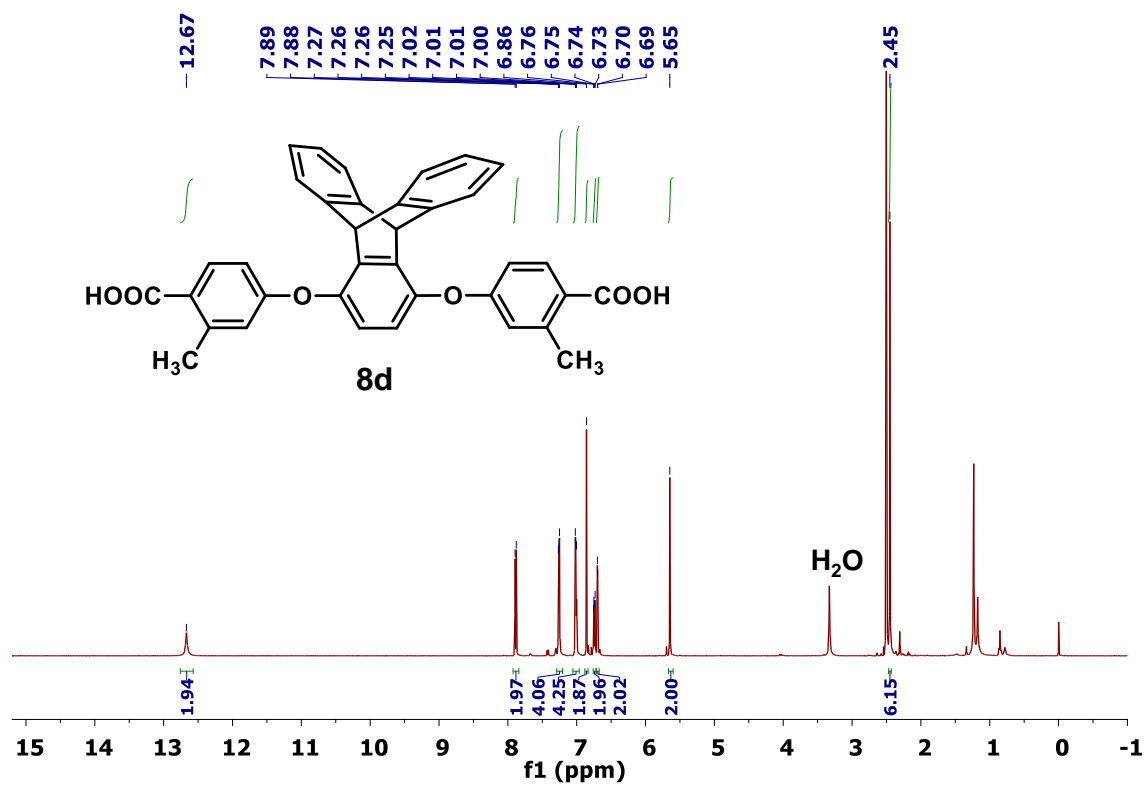


Figure S17. ¹H and ¹³C NMR spectra of Trip(CH₃)-COOH (**8d**). NMR solvent: DMSO-*d*₆.

Section S12. ^1H , ^{13}C CP-MAS NMR and FT-IR spectra of model compounds (M1&M2)

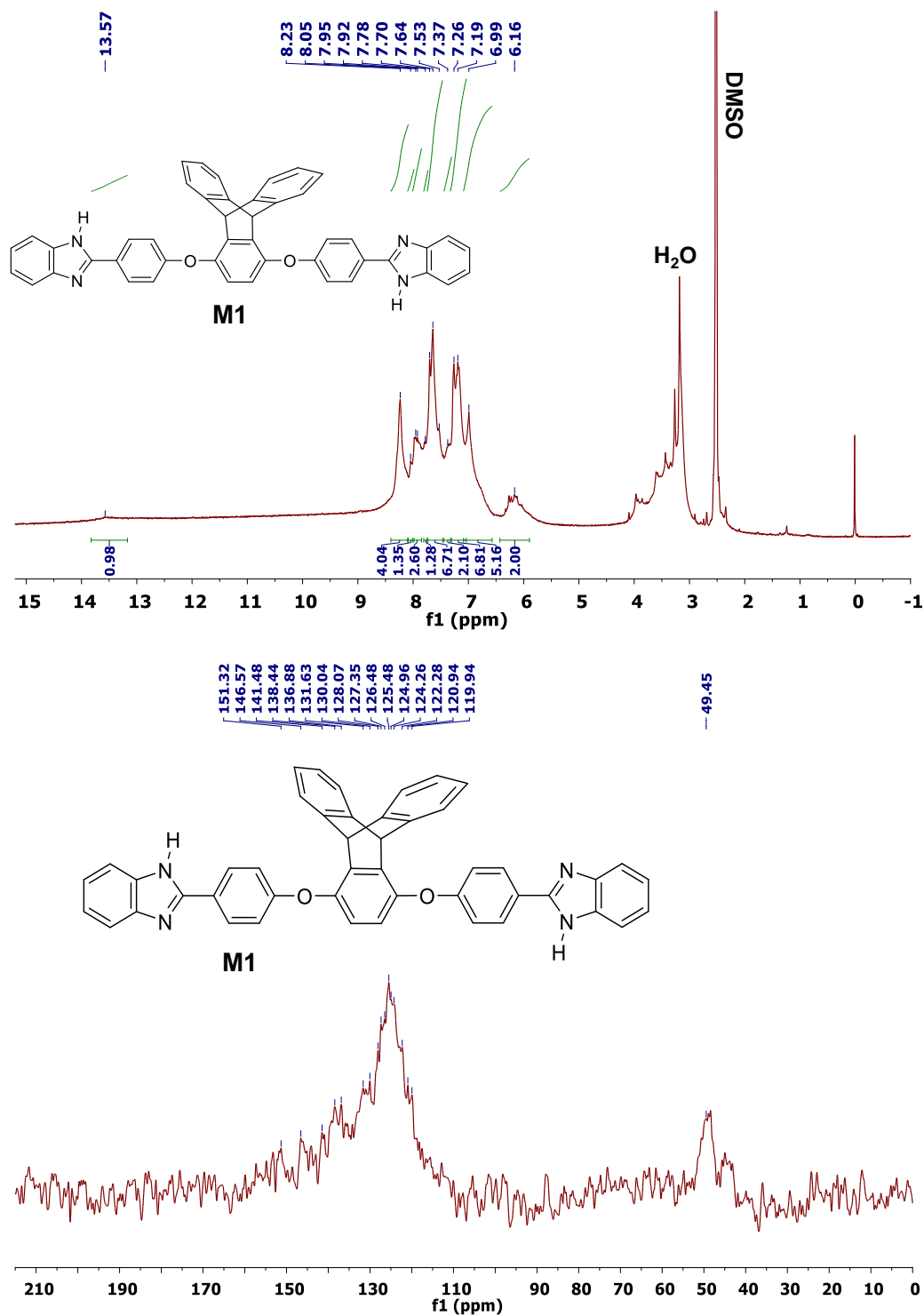


Figure S18. ^1H NMR spectra (solvent: DMSO- d_6) and ^{13}C CP-MAS solid-state NMR spectra of model compound (M1).

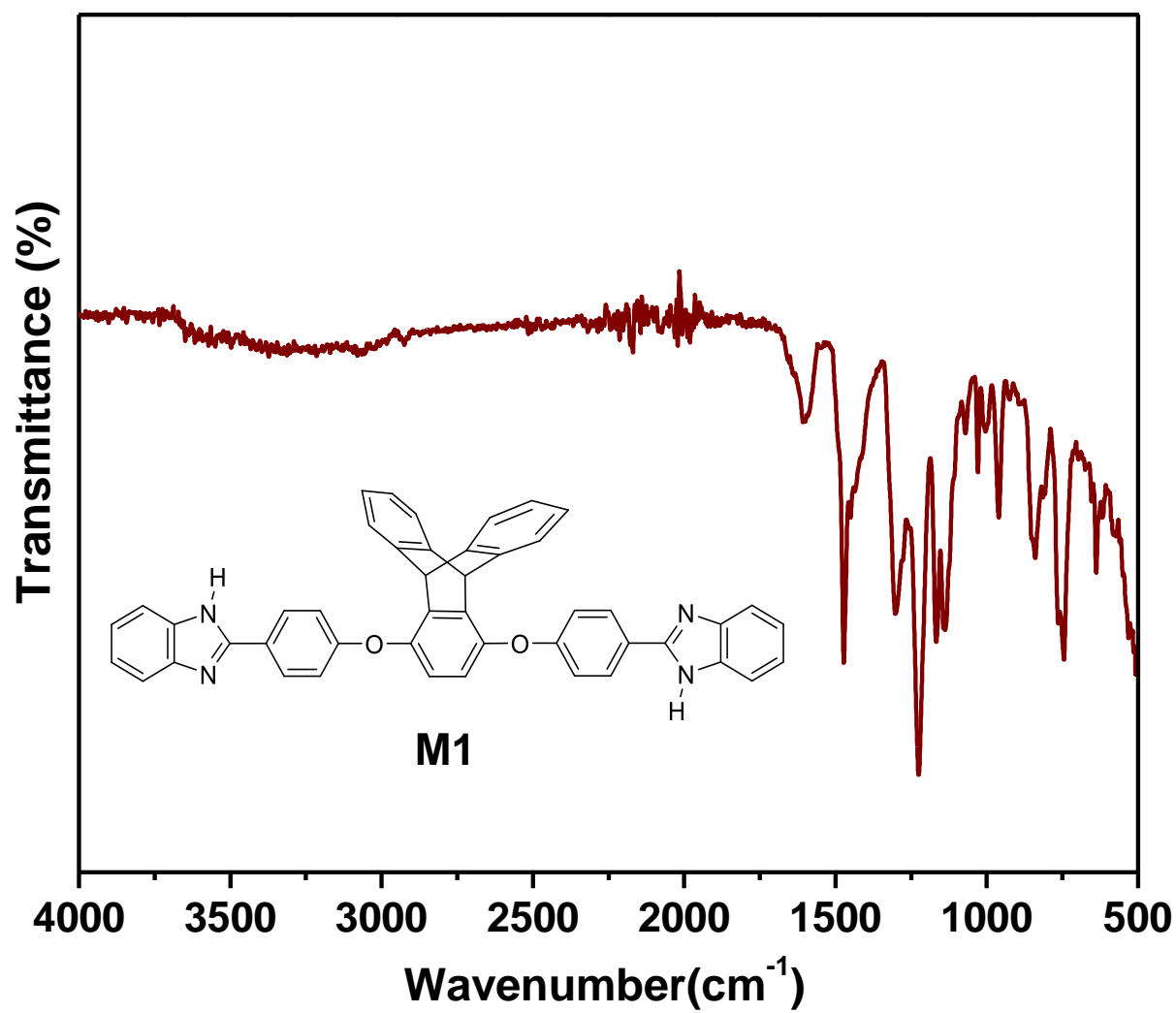


Figure S19. FTIR spectra of model compound (M1).

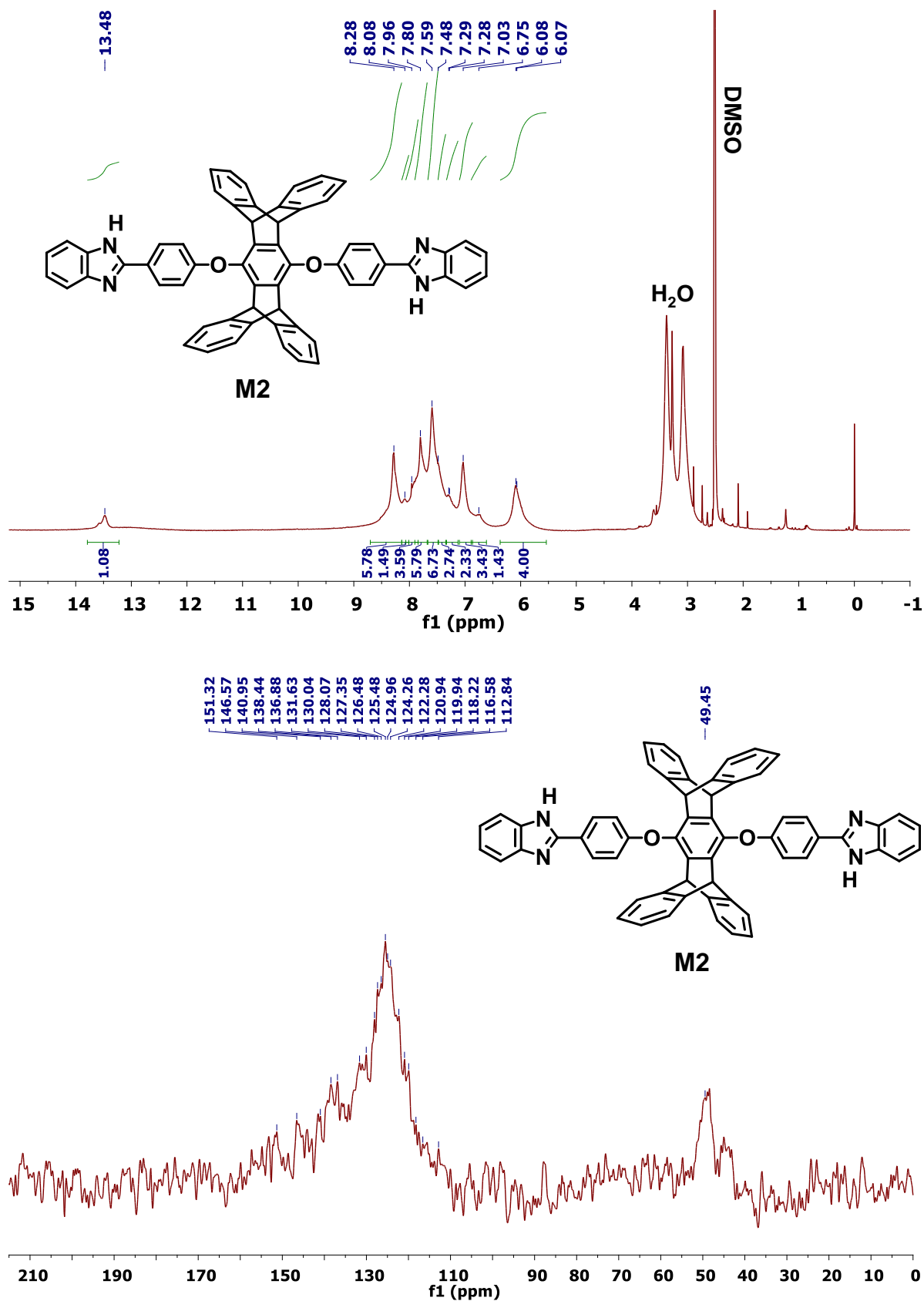


Figure S20. ¹H NMR spectra (solvent: DMSO-*d*₆) and ¹³C CP-MAS solid-state NMR spectra of model compound (M2).

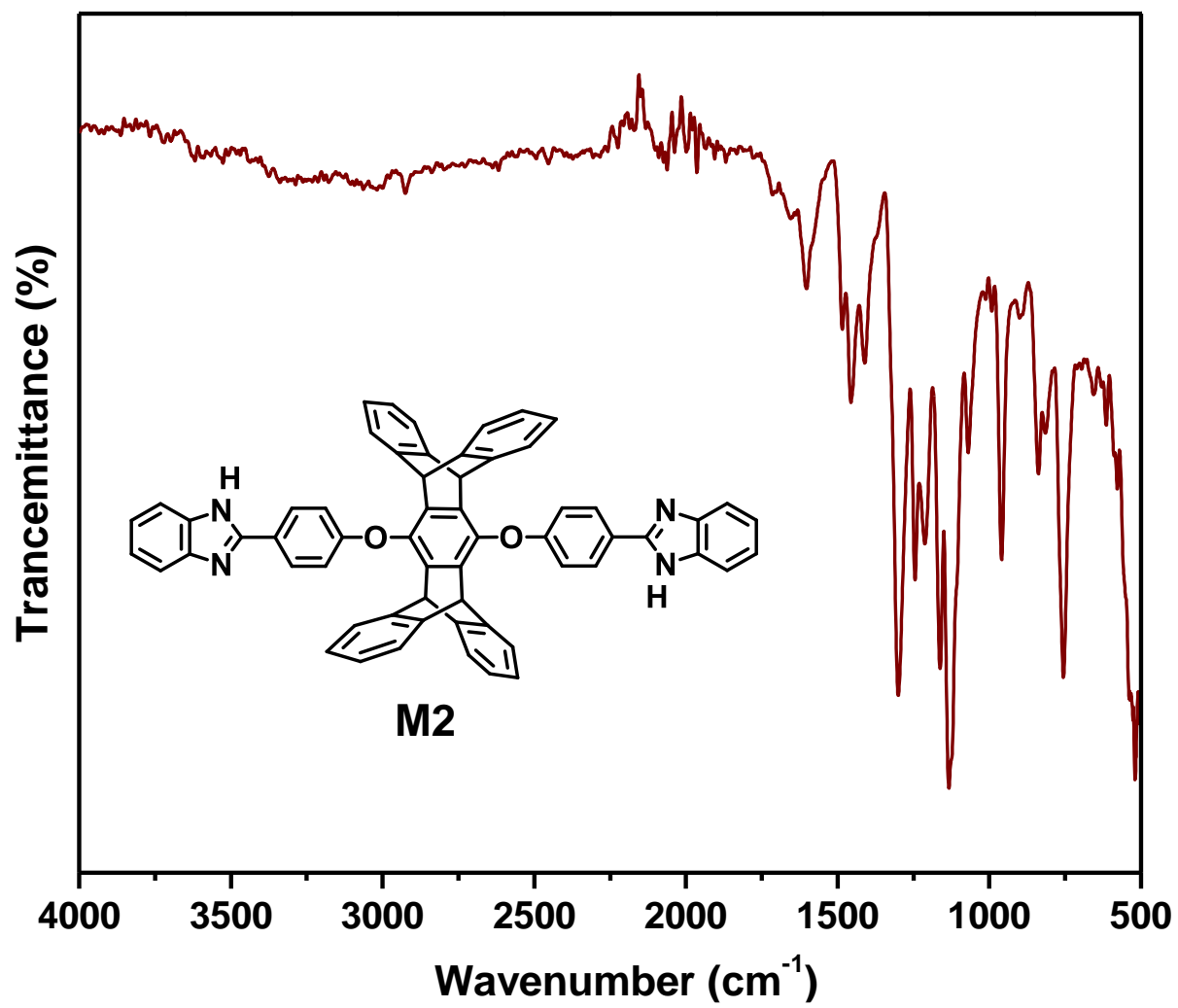


Figure S21. FTIR spectra of the model compound (M2).

Section 13. Hydrogen bonding network structures of of PenTrip-COOH and Trip-COOH

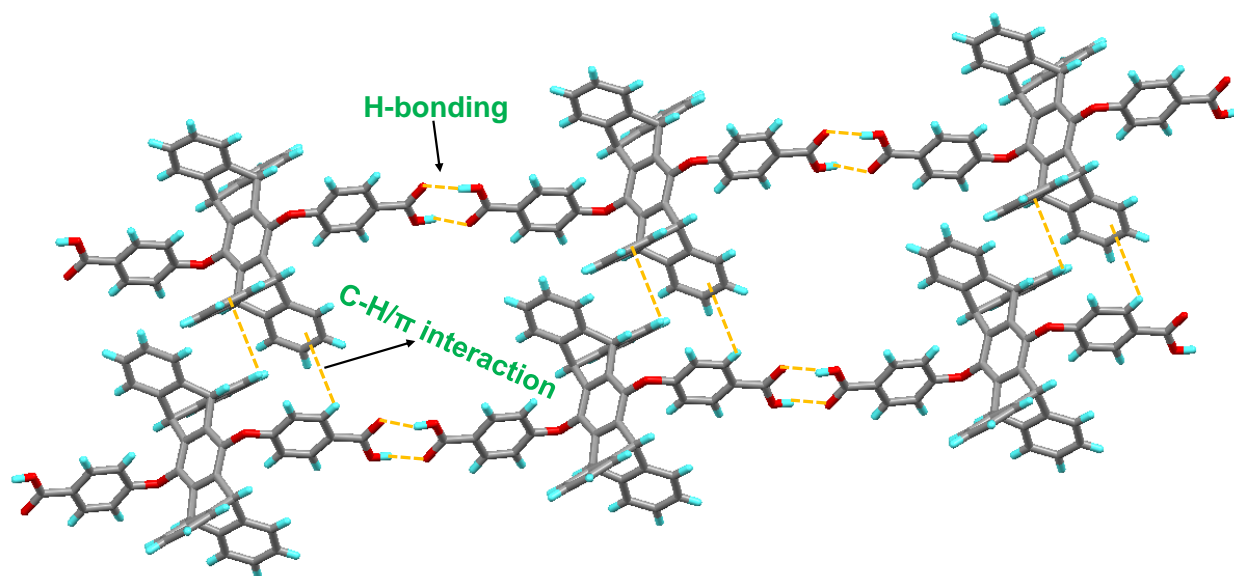


Figure S22. Adjacent building blocks of PenTrip-COOH forms the extended network and are held together by intermolecular hydrogen bonding (orange) involving the carboxylic groups and C-H... π stacking interactions. Grey-carbon, light blue-hydrogen, red-oxygen.

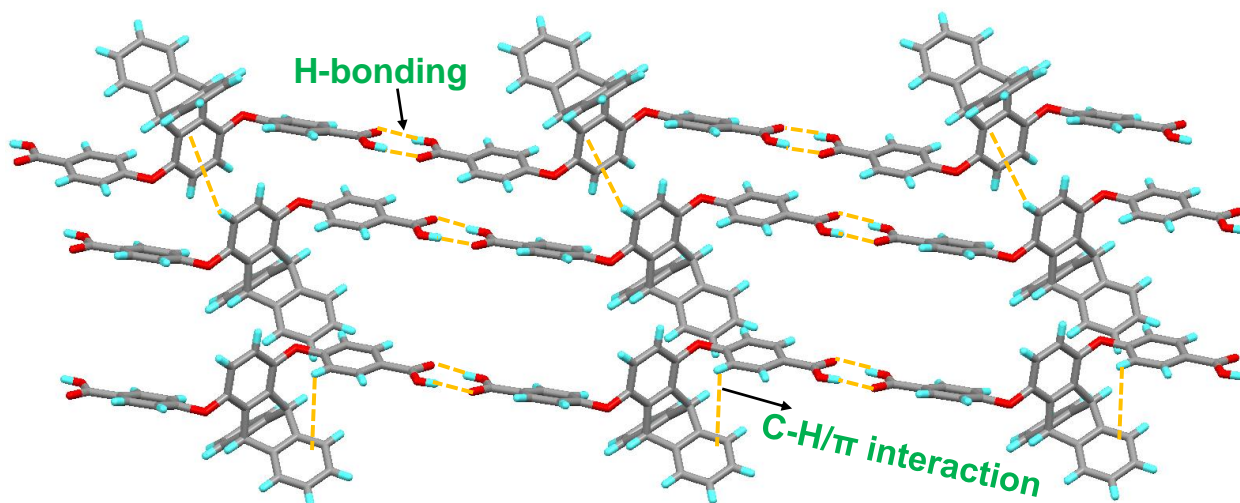


Figure S23. Adjacent building blocks of Trip-COOH forms the extended network and are held together by intermolecular hydrogen bonding (orange) involving the carboxylic groups and C-H... π stacking interactions. Grey-carbon, light blue-hydrogen, red-oxygen.

Section S14. ^{13}C CP-MAS NMR spectra of Trip-PyPBI and PenTrip-PyPBI

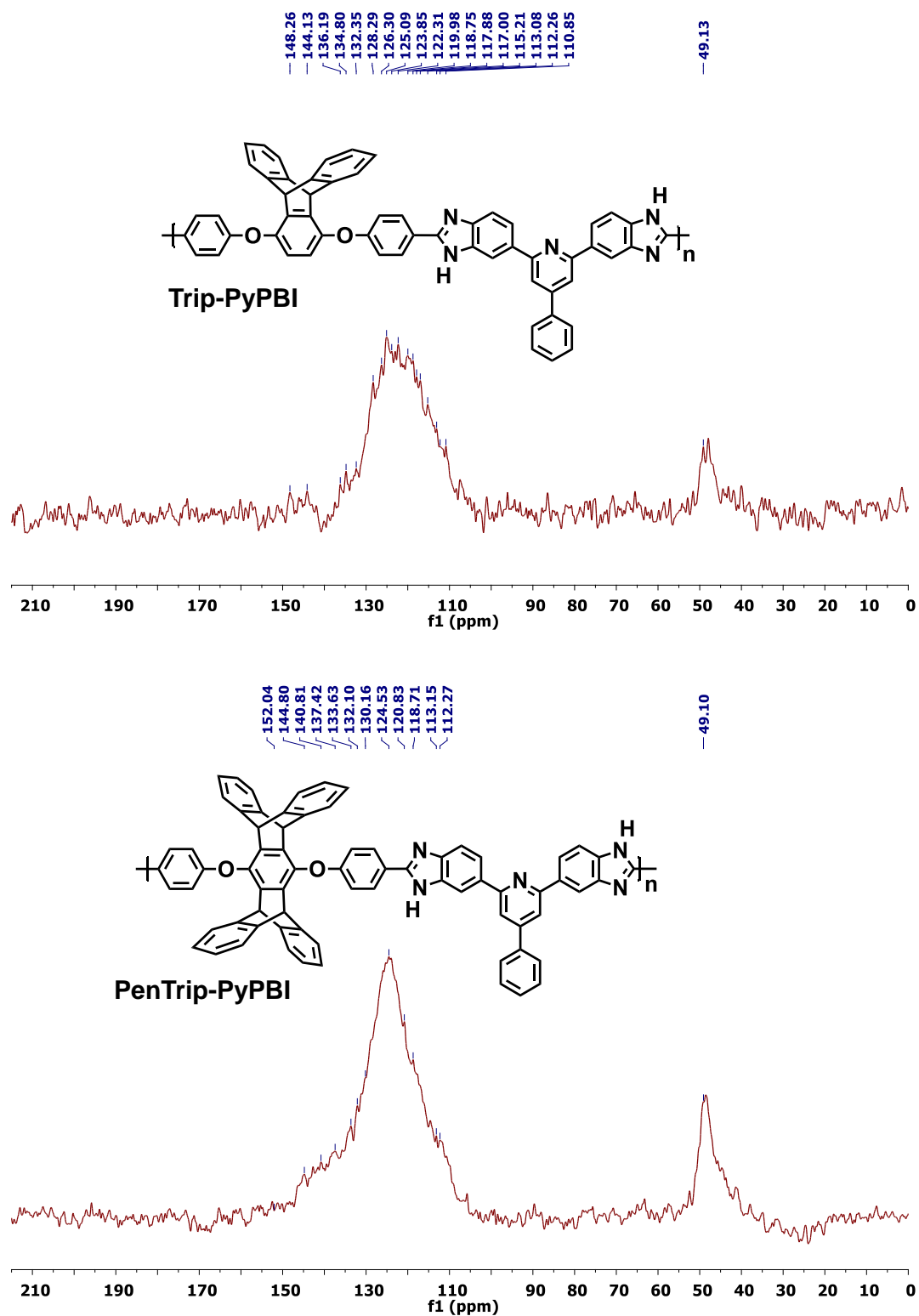


Figure S24. ^{13}C CP-MAS solid-state NMR spectra of Trip-PyPBI and PenTrip-PyPBI.

Section S15. XPS spectra of Trip-PyPBI and Trip(CH₃)-PyPBI

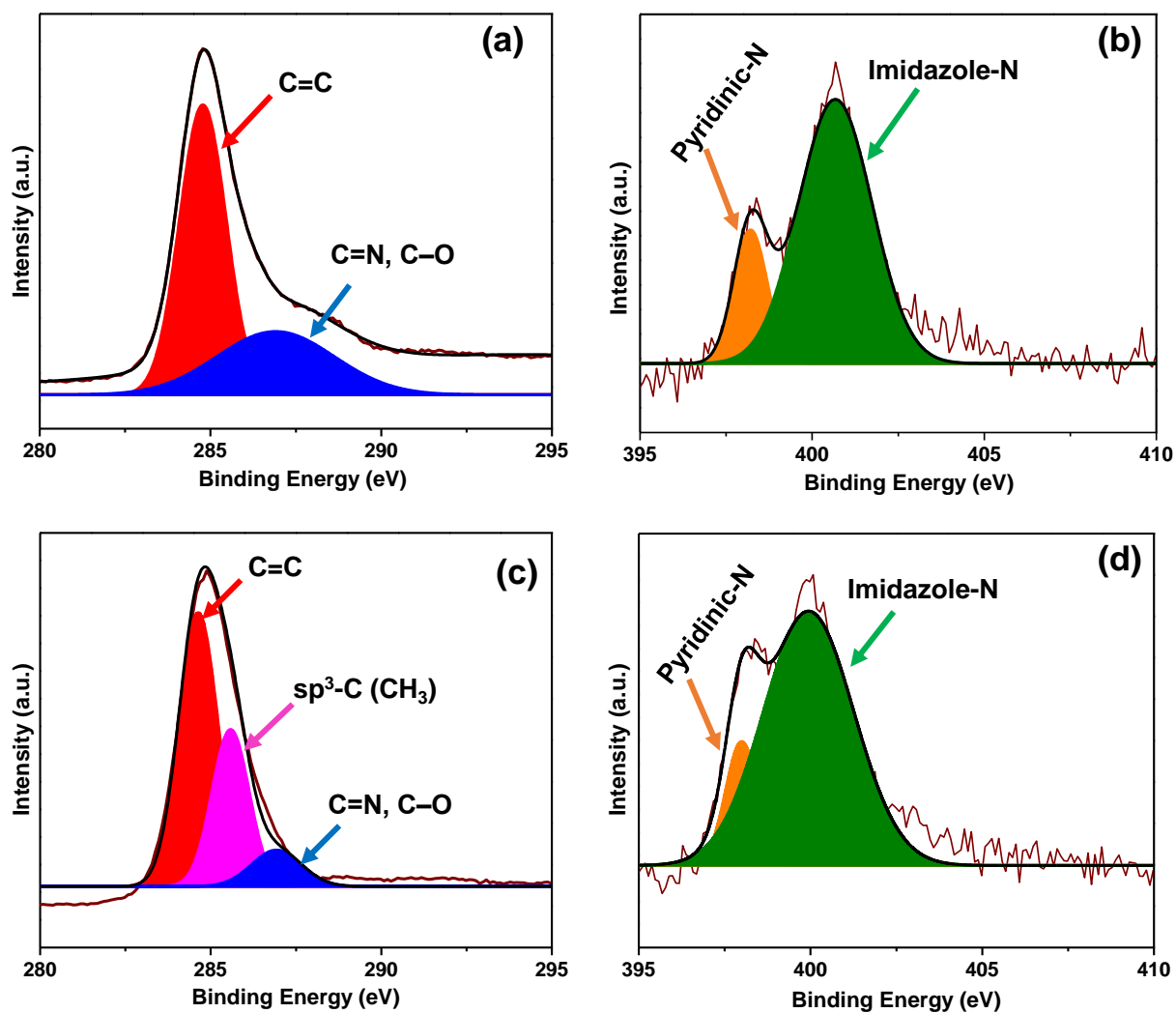


Figure S25. XPS spectra of C1s, N1s band of Trip-PyPBI (a & b) and Trip(CH₃)-PyPBI (c & d).

Section S16. Additional figures

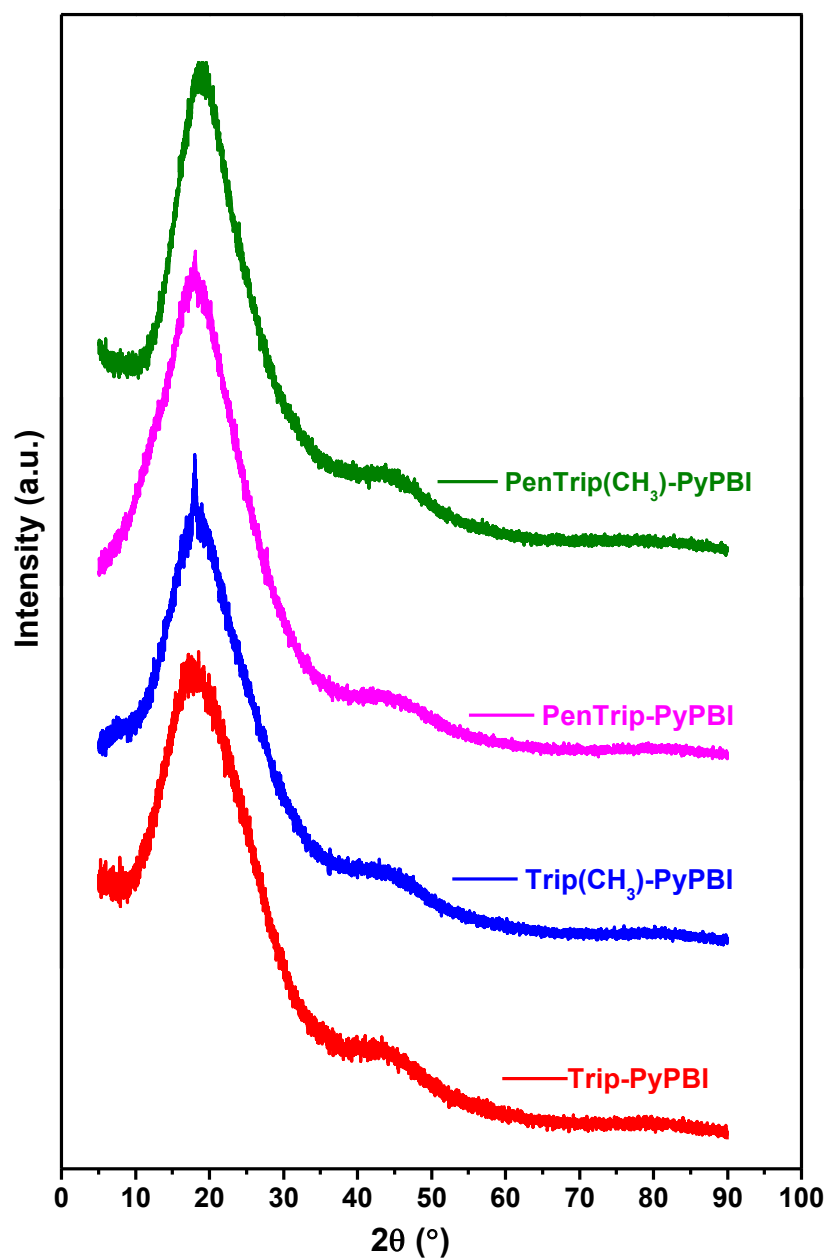


Figure 26. PXRD patterns of iptycene-based PyPBIs.

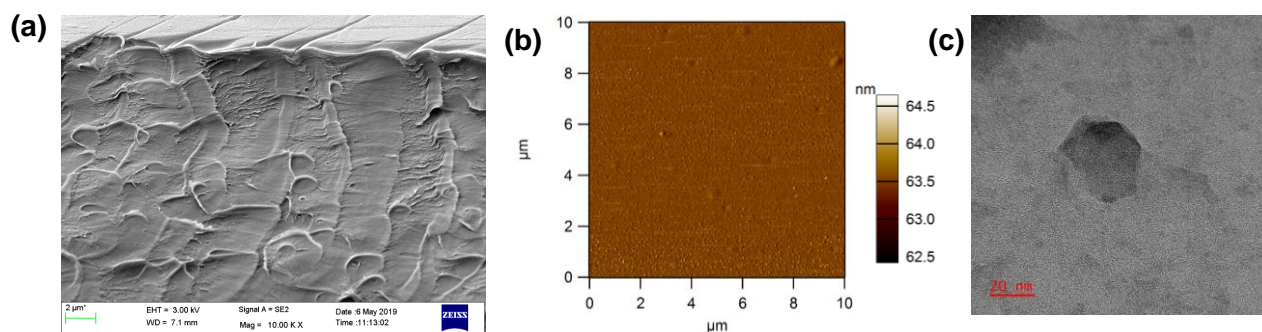


Figure 27. Microscopic morphologies Ph-PyOPBI membrane. (a) Cross-sectional FESEM, (b) AFM height and (c) HR-TEM Scale bar = 20 nm image.

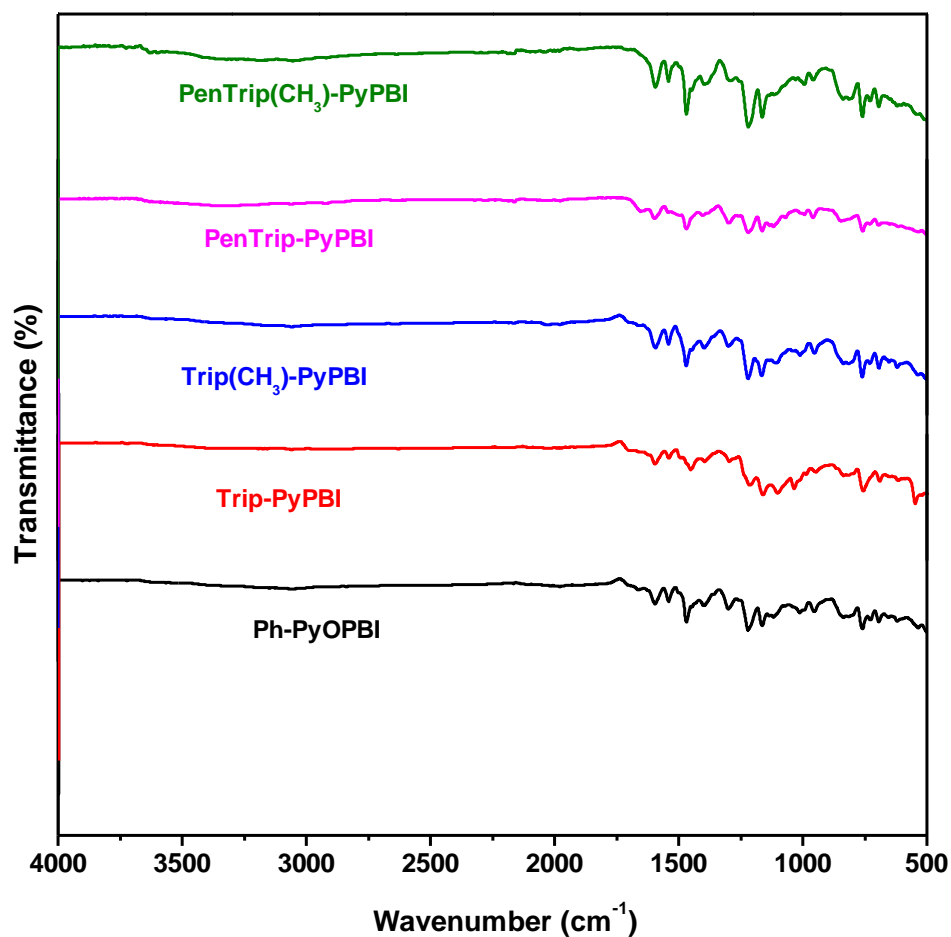


Figure S28. FTIR spectra of Ph-PyOPBI and iptycene-based PyPBIs after the treatment under harsh conditions for 6 days.

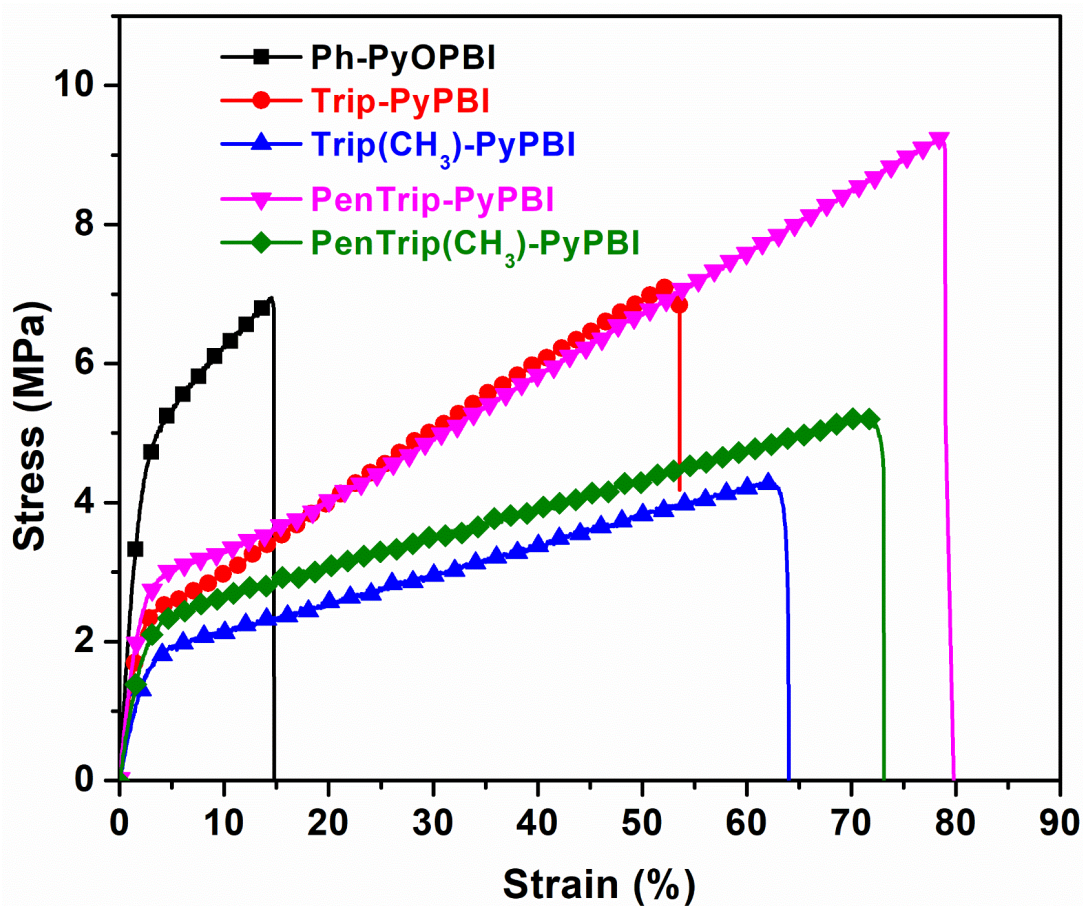


Figure S29. Stress–strain plots of doped Ph-PyOPBI and 3D iptycene-based PyPBI membranes.

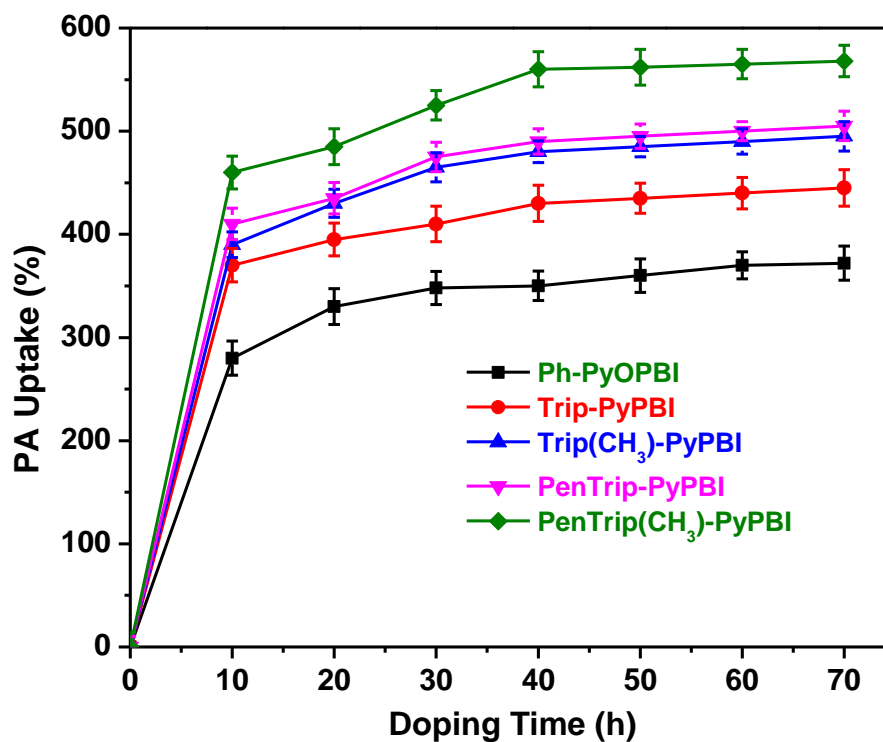


Figure S30. The PA uptake of different iptycene-based PyPBI membranes along with Ph-PyOPBI.

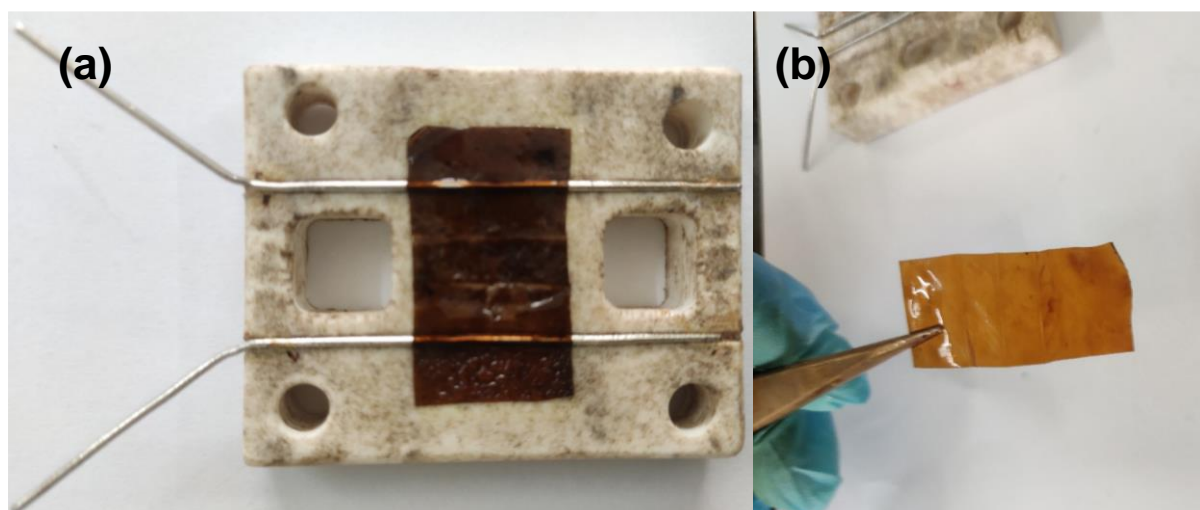


Figure S31. The PA-doped membrane mechanical integrity of PenTrip(CH₃)-PyPBI after proton conductivity measurement at 180 °C for 72 h. (a) Membrane in the cell with electrodes after measurement and (b) membrane taken out of the cell but still remain flexible to handle.

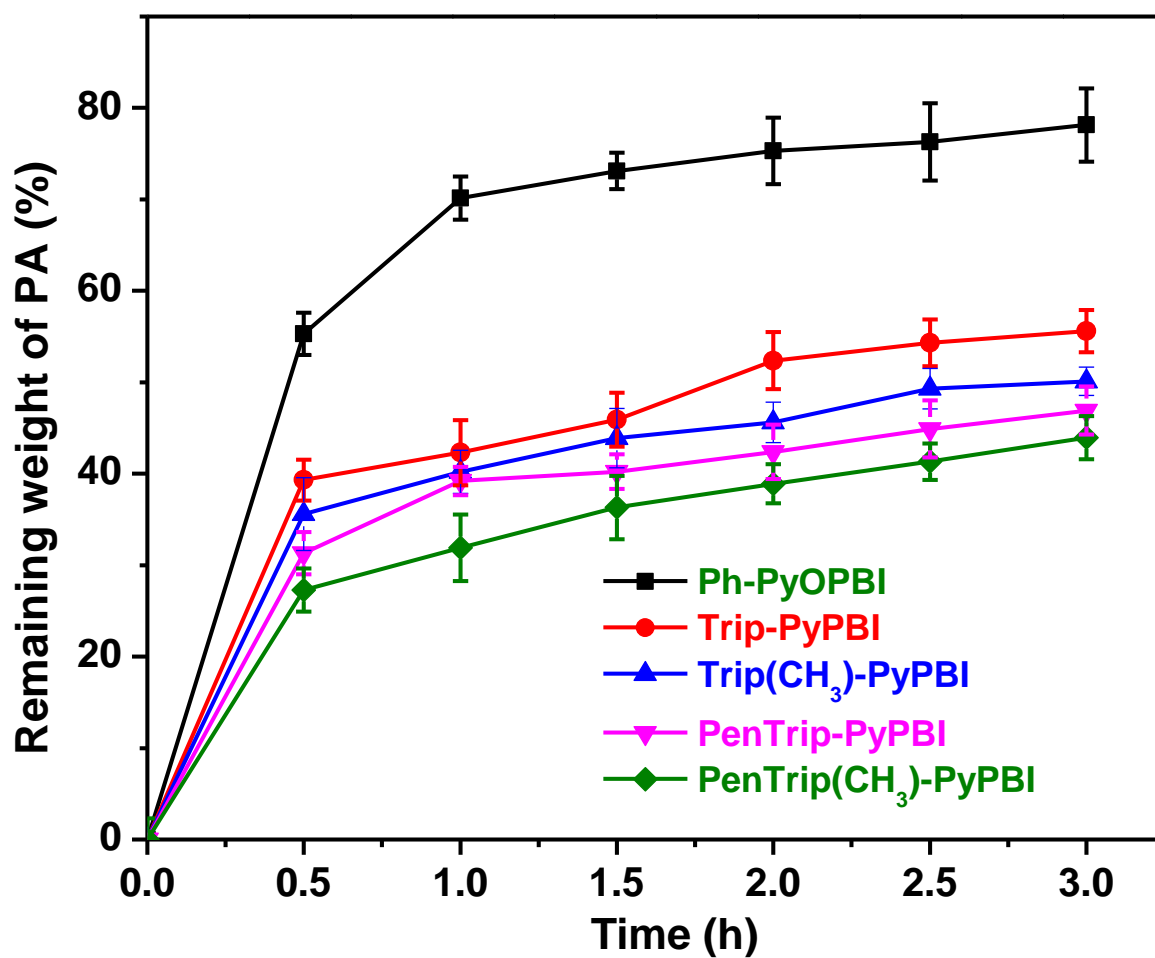


Figure S32. PA stability of different iptycene-based PyPBI membranes under the water vapour at ~ 100 °C.

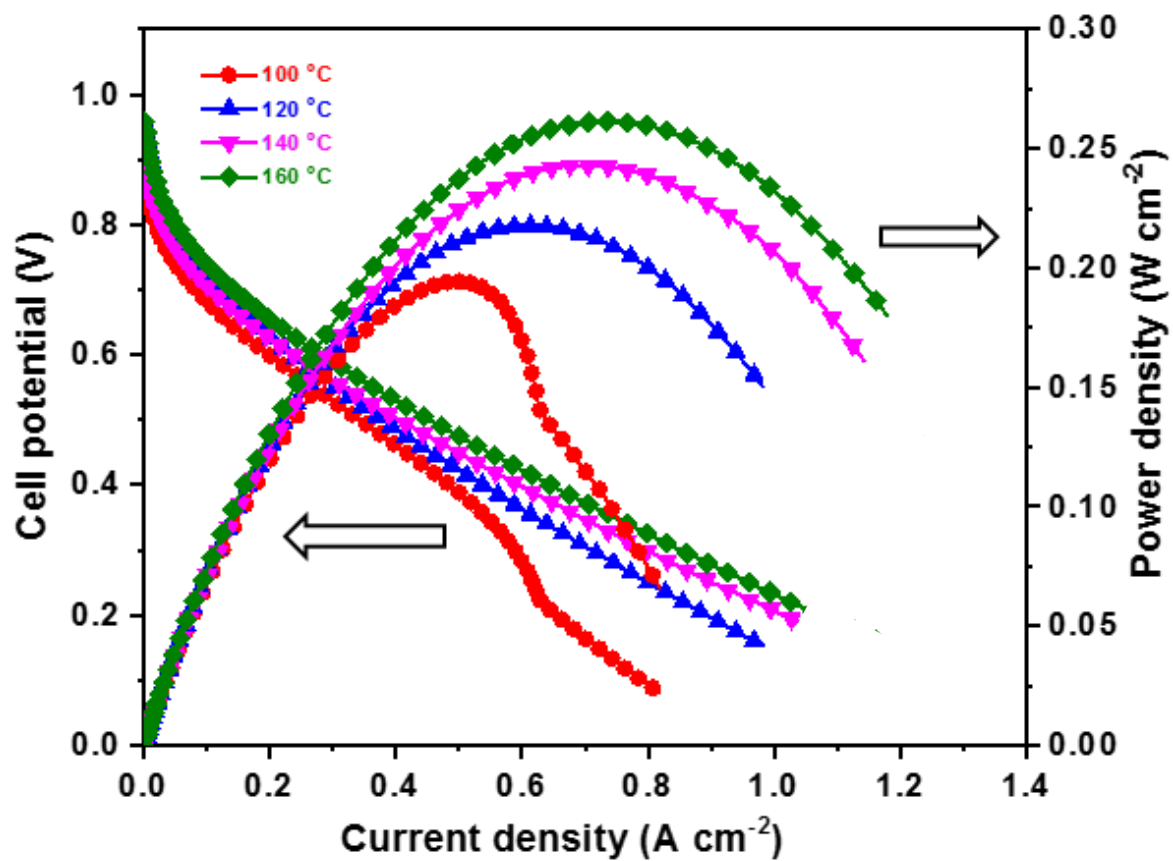
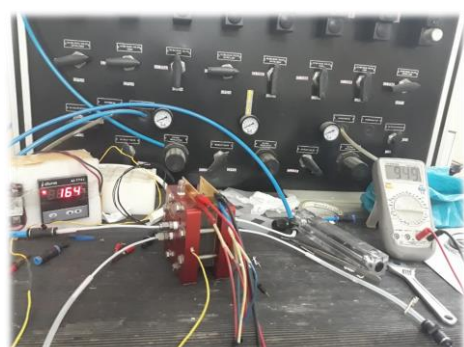


Figure S33. Polarization curves and power density curves of the single cell based on PenTrip(CH₃)-PyPBI/600 wt% PA under un-humidified H₂ and O₂ at various temperatures.



Fuel Cell

Trip(CH₃)-PyPBI



PenTrip(CH₃)-PyPBI



Figure S34. Photos of fuel cell, Trip(CH₃)-PyPBI and PenTrip(CH₃)-PyPBI assembled MEA after single cell test.

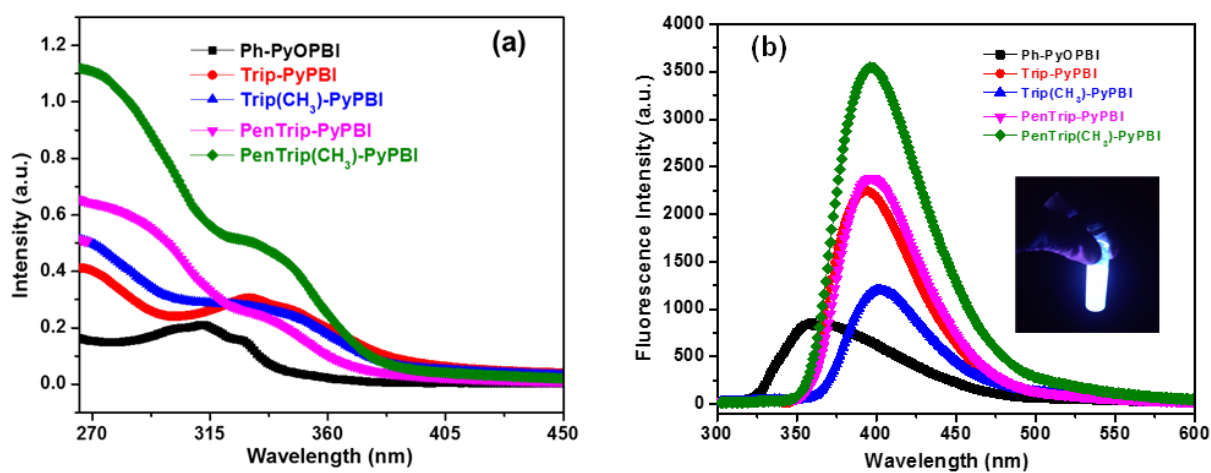


Figure S35. (a) Absorption spectra and (b) Fluorescence emission spectra of iptycene-based PyPBIs in DMSO dilute solution. Emission photographs of the corresponding solutions under 365 nm irradiation is also shown in the inset. Spectra were recorded by exciting the sample at 360 nm. Concentration of the solution was 2×10^{-5} M where molarity is calculated by considering repeat unit as 1 mol.

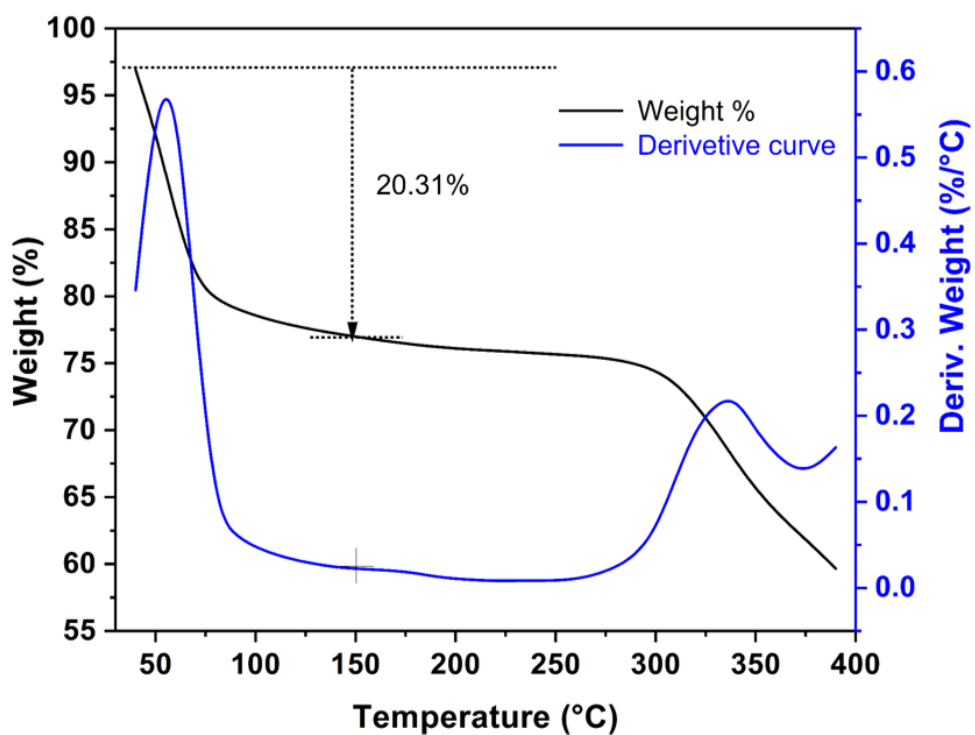


Figure S36. TGA curve of PenTrip-COOH (**4c**) measured under N₂. 20.31 wt% loss observed below 150 °C is due to the loss of the lattice 1, 4-dioxane molecules. Calcd. for PenTrip-COOH: 20.02%

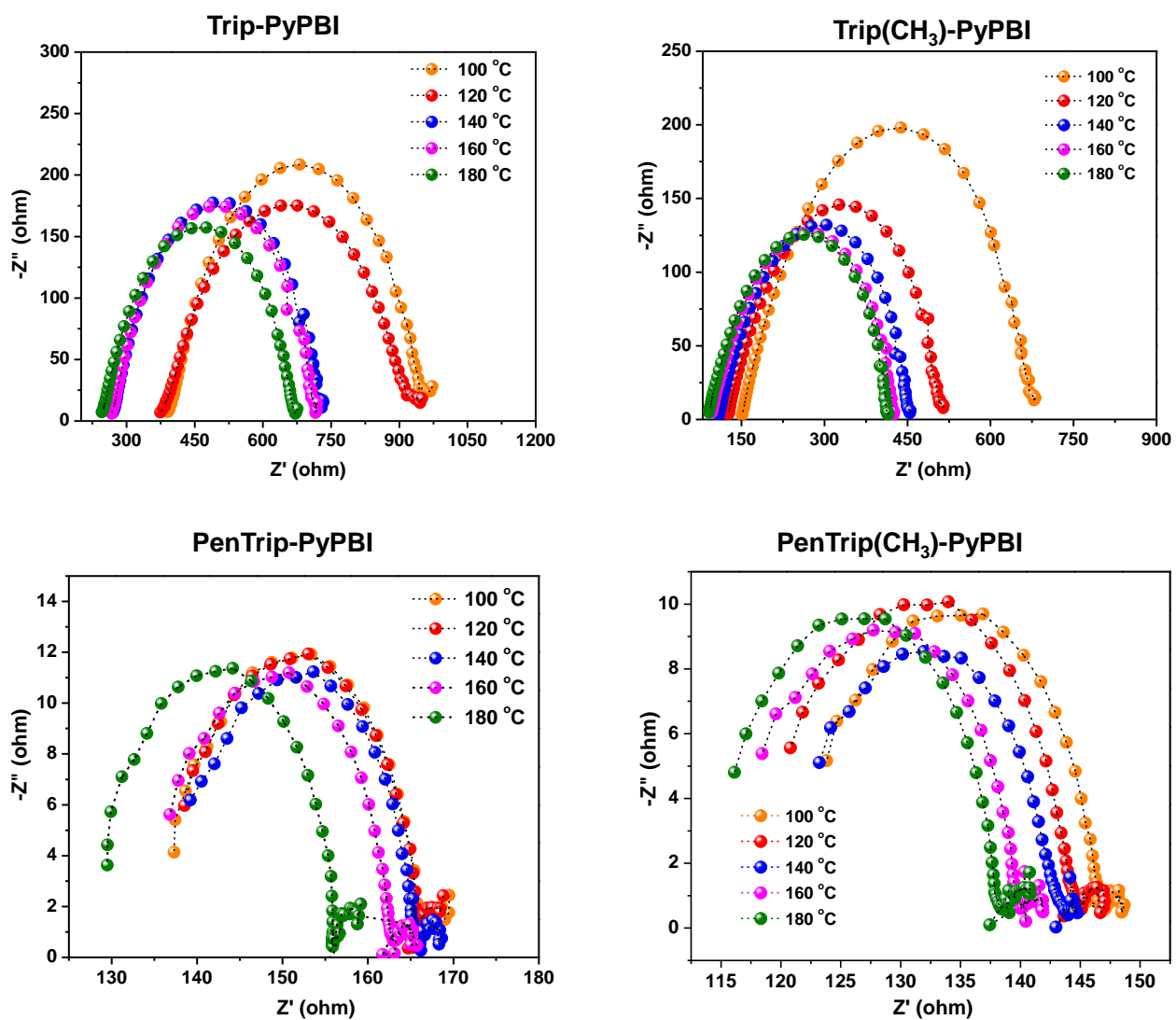


Figure S37. Nyquist plots at different temperatures for PA loaded Trip-PyPBI, Trip(CH₃)-PyPBI, PenTrip-PyPBI and PenTrip(CH₃)-PyPBI membranes.

Table S6. Comparison of the PA uptake, acid leaching and proton conductivity of the membranes prepared in this work with those of typical PBI-based PEMs reported in the literatures.

Samples	PA uptake		Conductivity (S cm ⁻¹)	PA leaching (wt%)	Conductivity Stability (S cm ⁻¹) at 160 °C	Ref.
	ADL	(wt%)				
PenTrip(CH ₃)-PyPBI	32	600	0.242 ^a	35.1	0.175	This study
PenTrip-PyPBI	28	573	0.196 ^a	40.1	0.163	This study
Trip(CH ₃)-PyPBI	25	446	0.162 ^a	46.2	0.137	This study
Trip(CH ₃)-PyPBI	20	489	0.138 ^a	50.6	0.123	This study
Ph-PBI	14.6	253	0.126 ^b	-	-	[8]
Me-PBI	20.6	-	0.165 ^b	-	0.06	[9]
Ph(CF ₃)-PyOPBI	22.1	492	0.078 ^a	28	0.048	[10]
PyOPBI	~12	~298	0.007 ^a	38	0.005	[10]
F ₆ -PBI	8.8	-	0.064 ^a	-	-	[11]
Porous OPBI	9.6	-	0.078	-	-	[12]
m-PBI	4	132	0.048 ^a	~45	-	[13]
<i>p</i> -PBI	4.7	-	0.018 ^a	-	-	[14]
P0.5-b-O0.5-PBI	7.9	-	~0.12	-	-	[14]
OPBI	~8.2	~200	~0.08 ^b	30.9 wt%	~0.07	[15]
CrL-PBI	~25	~620	0.137 ^b	16 wt%	~0.08	[15]
pPBI-50	9.1	290	0.048 ^b	-	-	[16]
ABPBI	3.6	-	0.024 ^a	-	-	[17]
ph-PBI	8	-	0.011 ^c	15 wt%	-	[18]

^a 180 °C, ^b 200 °C, ^c 140 °C

Section S17. REFERENCE

1. S. Maity and T. Jana, *Macromolecules*, 2013, **46**, 6814-6823.
2. Sheldrick, G. M. *SHELXL. Program for Refinement of Crystal Structures*; Universitat Goettingen: Germany, 2014.
3. F. Gong, H. Mao, Y. Zhang, S. Zhang and W. Xing, *Polymer*, 2011, **52**, 1738-1747.
4. S. Luo, J. Liu, H. Lin, B. A. Kazanowska, M. D. Hunckler, R. K. Roeder and R. Guo, *J. Mater. Chem. A*, 2016, **4**, 17050-17062.
5. P. E. Eaton, G. R. Carlson and J. T. Lee, *J. Org. Chem.*, 1973, **38**, 4071-4073.
6. Y. Yuan, F. Johnson and I. Cabasso, *J. Appl. Polym. Sci.*, 2009, **112**, 3436-3441.
7. Harilal, R. Nayak, P. C. Ghosh and T. Jana, *ACS Appl. Polym. Mater.*, 2020, **2**, 3161-3170.
8. X. Li, H. Ma, P. Wang, Z. Liu, J. Peng, W. Hu, Z. Jiang, B. Liu and M. D. Guiver, *Chem. Mater.*, 2020, **32**, 1182-1191.
9. X. Li, H. Ma, Y. Shen, W. Hu, Z. Jiang, B. Liu and M. D. Guiver, *J. Power Sources*, 2016, **336**, 391-400.
10. Harilal, A. Shukla, P. C. Ghosh and T. Jana, *ACS Appl. Energy Mater.*, 2021, **4**, 1644-1656.
11. J. Yang, Q. Li, L. N. Cleemann, J. O. Jensen, C. Pan, N. J. Bjerrum and R. He, *Adv. Energy Mater.*, 2013, **3**, 622-630.
12. K. Geng, H. Tang, Q. Ju, H. Qian and N. Li, *J. Membr. Sci.*, 2021, **620**, 118981.
13. S. Zhou, J. Guan, Z. Li, L. Huang, J. Zheng, S. Li and S. Zhang, *J. Mater. Chem. A*, 2021, **9**, 3925-3930.
14. L. Wang, Z. Liu, J. Ni, M. Xu, C. Pan, D. Wang, D. Liu and L. Wang *J. Membr. Sci.*, 2019, **572**, 350-357.

15. P. Wang, J. Peng, B. Yin, X. Fu, L. Wang, J.-L. Luo and X. Peng, *J. Mater. Chem. A*, 2021, **9**, 26345-26353.
16. S. Wang, C. Zhao, W. Ma, G. Zhang, Z. Liu, J. Ni, M. Li, N. Zhang and H. Na, *J. Membr. Sci.*, 2012, **411**, 54-63.
17. S. S. Rao, V. R. Hande, S. M. Sawant, S. Praveen, S. K. Rath, K. Sudarshan, D. Ratna and M. Patri, *ACS Appl. Mater. Interfaces*, 2019, **11**, 37013-37025.
18. M. R. Berber and N. Nakashima, *ACS Appl. Mater. Interfaces*, 2019, **11**, 46269-46277.